Appendix A.31:

Mark Treffers Dr – CPT 62594

Table 1: Site Description for Mark Treffers Dr (CC LIQ 28 – CPT 62594).

Attribute	Yes/No			Description/Date	Symbol in Figure 1
	10-m Buffer	20-m Buffer	50-m Buffer		
Near a body of surface water or other free face features?	No	No	No	The center of the site is ~200 m to the NE from the unnamed pond and ~580 m to the E from Travis Wetland, whose free-face heights are ~1-1.5 m. The Avon River is ~1200 m to the S of the center of the site. Its free-face height is ~1 m.	NA
Lateral spreading observed during the CES?	No	No	No	No ground cracks were observed by the mapping team.[1]	NA
Nearby buildings or structures?	No	No	No	NA	NA
Sloping land?	No	No	No	Flat, open field.	NA
Step changes in the ground surface?	No	No	No	NA	NA
Retaining walls?	No	No	No	NA	NA
Vegetation?	No	No	Yes	Trees and bushes cover 7% of the 50-m buffer and are in its SW and NE quadrants.	White Fill + Green Outline
Anthropogenic changes to the site between the LiDAR surveys?	No	Yes	Yes	The foot path in the S portion of the 50-m buffer existed from Dec 2004 through Feb 2006. The SE quadrant of the 50-m buffer had vegetation from Apr 2005 through Feb 2006.	NA
Other important factors?	Yes	Yes	Yes	The soccer field covers 100, 100, and 79% of the 10-, 20-, and 50-m buffers, respectively, and has two movable soccer goals.	NA

Notes: Buffer is the area within a circle of a specified radius with CPT investigations done at its center (172.708784°, -43.491115°); The July 2003 LiDAR survey should not be used in the settlement analysis due to the anthropogenic changes that occurred prior to the Sep 2010 earthquake.

[1] Canterbury Geotechnical Database. (2012). "Observed Ground Crack Locations", Map Layer CGD0400 - 23 July 2012, retrieved July 09, 2018 from https://canterburygeotechnicaldatabase.projectorbit.com/

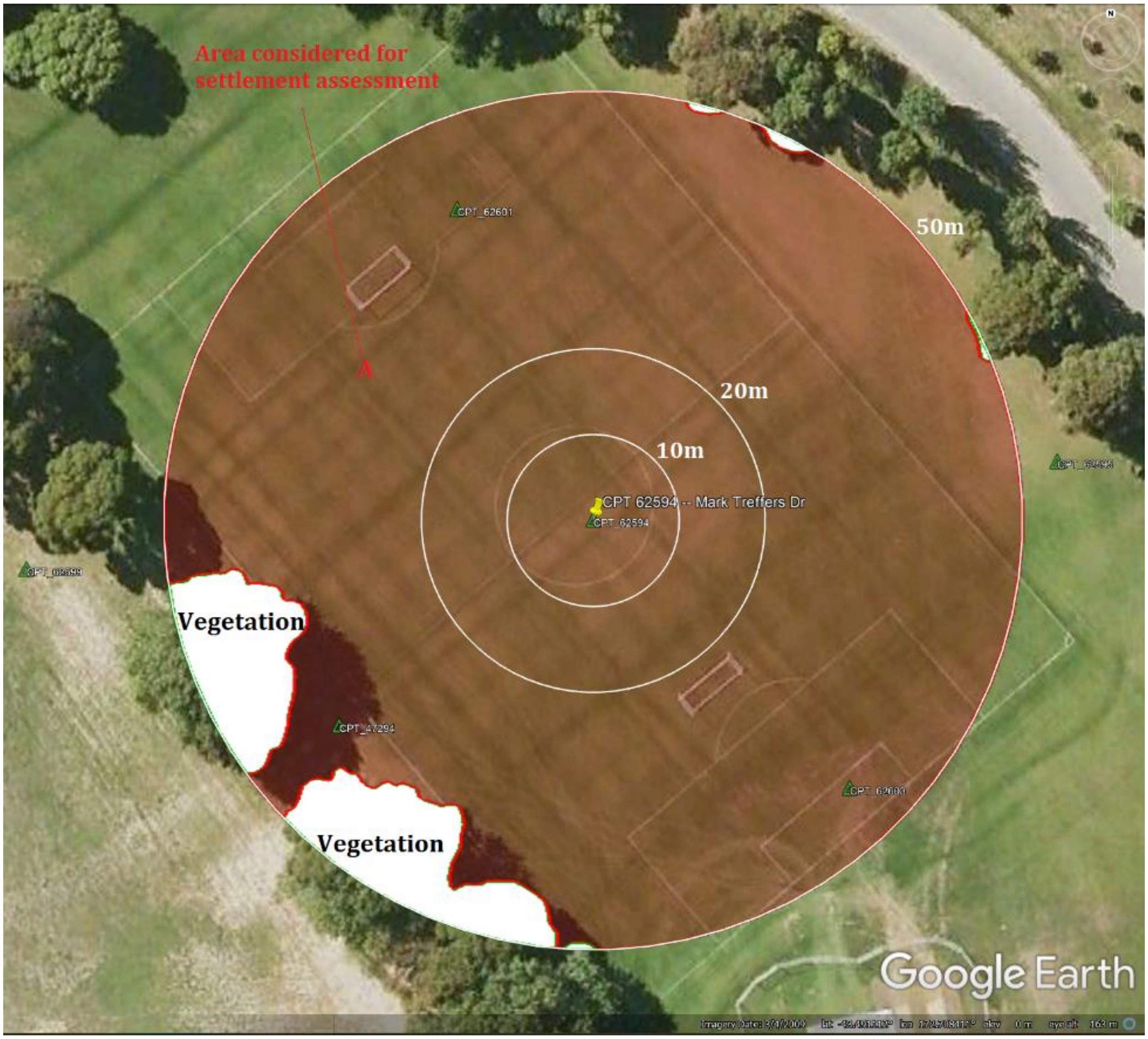

Figure 1: Site plan with areas where ejecta-settlement is considered.

Note 1: Patch A (outlined in red) in the free field was selected for detailed settlement assessment as an area free of vegetation and structures. Other important factors for the patch selection were its proximity to a CPT, a property subjected to addition and/or demolition of a structure, and front yard/backyard alterations (e.g., ploughing, rubble, scrap), and aerial distribution of sediment ejecta. The LiDAR-based settlement analyses were not performed for the Sep-11 EQ due to the evident absence of ejecta from Patch A and the anthropogenic changes.

Table 2: LiDAR flight error adjustments, global adjustments for the difference between average LiDAR point elevations and benchmark survey elevations, and vertical tectonic movement adjustments.

	Adjustments (mm)		
Earthquake Event(s)	LiDAR Flight Error	Global Offset[2]	Tectonic Vertical Movement
Sep-10	0	-3	0
Feb-11	0	16	-30
Jun-11	0	38	-45
Dec-11	0	-65	0
CES	0	-14	-75
Any LiDAR survey affected by ejecta?			No

Note: The negative sign indicates the subtraction from the ground surface subsidence, while the positive sign indicates the addition to the ground surface subsidence.

Table 3: LiDAR Measurement Error for Patch A.

Surveys	Buffer	Area Averaged Difference Indicating Repeat Measurement Error (mm)	$\sigma^*_{\text{individual LiDAR points}}$ (mm)	%Reduction in σ due to Area Averaging of LiDAR Points
Post Feb 2011: Mar 2011 and May 2011	10-m	NA	59	[NA,NA]
	20-m	NA		
	50-m	NA		
Post Dec 2011: Feb 2012 and Oct 2015	10-m	29	70	[40,47]
	20-m	33		
	50-m	28		

*Standard deviation; NA = Not available (no Mar 2011 LiDAR survey).

[2] Russell, J., & van Ballegooy, S. (2015). *Canterbury Earthquake Sequence: Increased liquefaction vulnerability assessment methodology*. New Zealand: Tonkin & Taylor Ltd.

Table 4: Ground surface subsidence adjustments due to LiDAR measurement error for Patch A.

Earthquake Event(s)	$\sigma_{\text{pre-EQ LiDAR survey}}$ (mm)	$\sigma_{\text{post-EQ LiDAR survey}}$ (mm)	σ_{total} (mm)	Area Average Adjusted σ (mm) **
Sep-10	158	56	134	±63
Feb-11	56	59	59	±28
Jun-11	59	61	62	±29
Dec-11	61	70	87	±41
CES	158	70	124	±59

**Based on the highest %Reduction in Table 3a.

Table 5: Raw liquefaction-related ground surface subsidence using original LiDAR points for Patch A.

	Average Ground Surface Subsidence (mm)		
Earthquake Event(s)	10-m Buffer	20-m Buffer	50-m Buffer
Sep-10	ND	ND	ND
Feb-11	248	232	219
Jun-11	83	80	77
Dec-11	91	83	71
CES	ND	ND	ND

ND = Not determined.

Table 6: Corrected liquefaction-related ground surface subsidence using original LiDAR points for Patch A with the calculated adjustments in Table 2.

	Average Calculated Ground Surface Subsidence (mm)		
Earthquake Event(s)	10-m Buffer	20-m Buffer	50-m Buffer
Sep-10	ND	ND	ND
Feb-11	234±25	218±25	205±25
Jun-11	76±25	73±25	70±25
Dec-11	26±50	18±50	6±50
CES	ND	ND	ND

Notes: Plus/minus values are same as those in Table 4a, but rounded to the nearest 25; Positive overall values indicate ground surface subsidence, while negative overall values indicate ground surface uplift; ND = Not determined.

Table 7: Corrected liquefaction-related ground surface subsidence for Patch A using LiDAR DEMs.

	Estimated Ground Surface Subsidence (mm)								
	10-m Buffer			20-m Buffer			50-m Buffer		
Earthquake Event(s)	16th %ile	50th %ile	84th %ile	16th %ile	50th %ile	84th %ile	16th %ile	50th %ile	84th %ile
Sep-10	ND	ND	ND	ND	ND	ND	ND	ND	ND
Feb-11	150	200	250	150	150	250	150	150	250
Jun-11	50	50	50	50	50	50	50	50	50
Dec-11	50	50	150	50	50	150	50	50	150
CES	ND	ND	ND	ND	ND	ND	ND	ND	ND

Notes: These percentiles are not the exact statistical measures; they indicate the spatial variability of ground surface subsidence; ND = Not determined due to the anthropogenic changes prior to the Sep 2010 LiDAR survey.

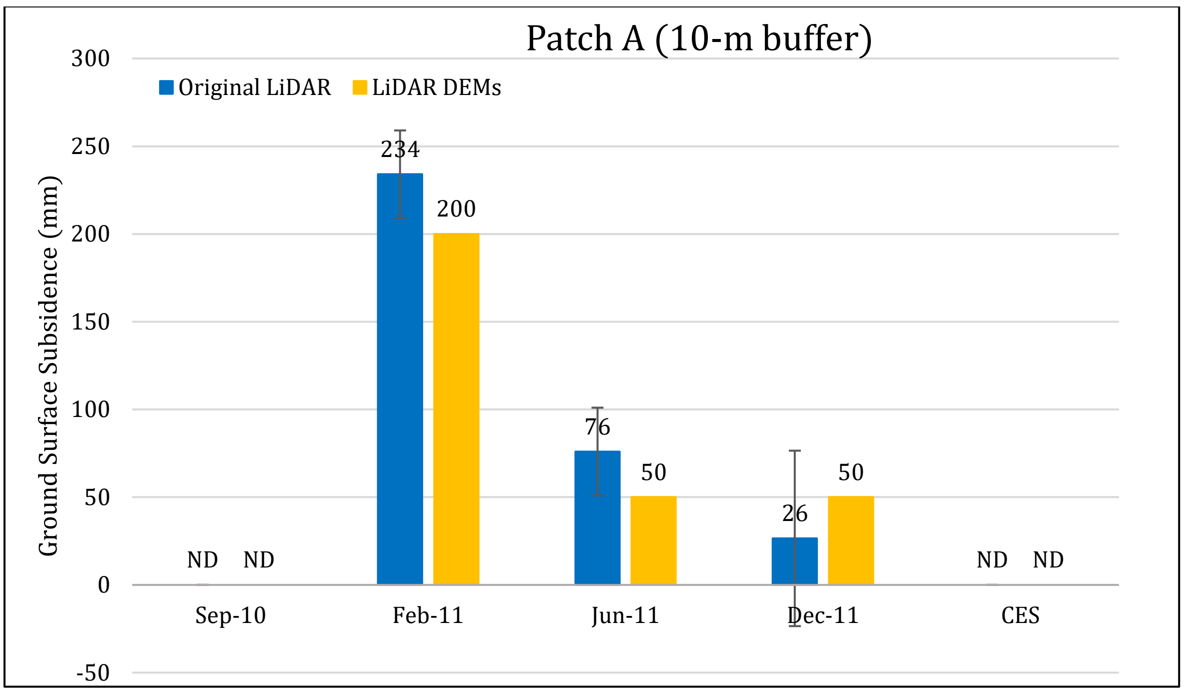

Figure 2: Comparison between ground surface subsidence determined from original LiDAR survey points and ground surface subsidence (50th %ile) estimated using LiDAR DEMs for Patch A (10-m buffer).

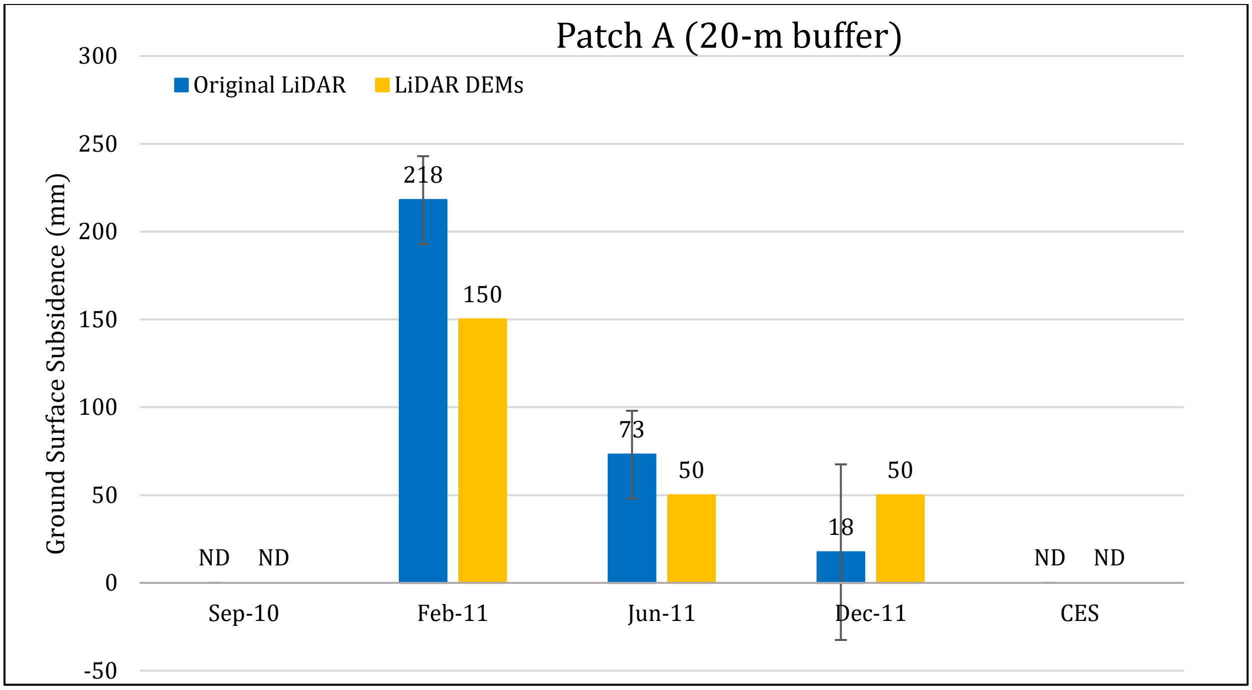

Figure 3: Comparison between ground surface subsidence determined from original LiDAR survey points and ground surface subsidence (50th %ile) estimated using LiDAR DEMs for Patch A (20-m buffer).

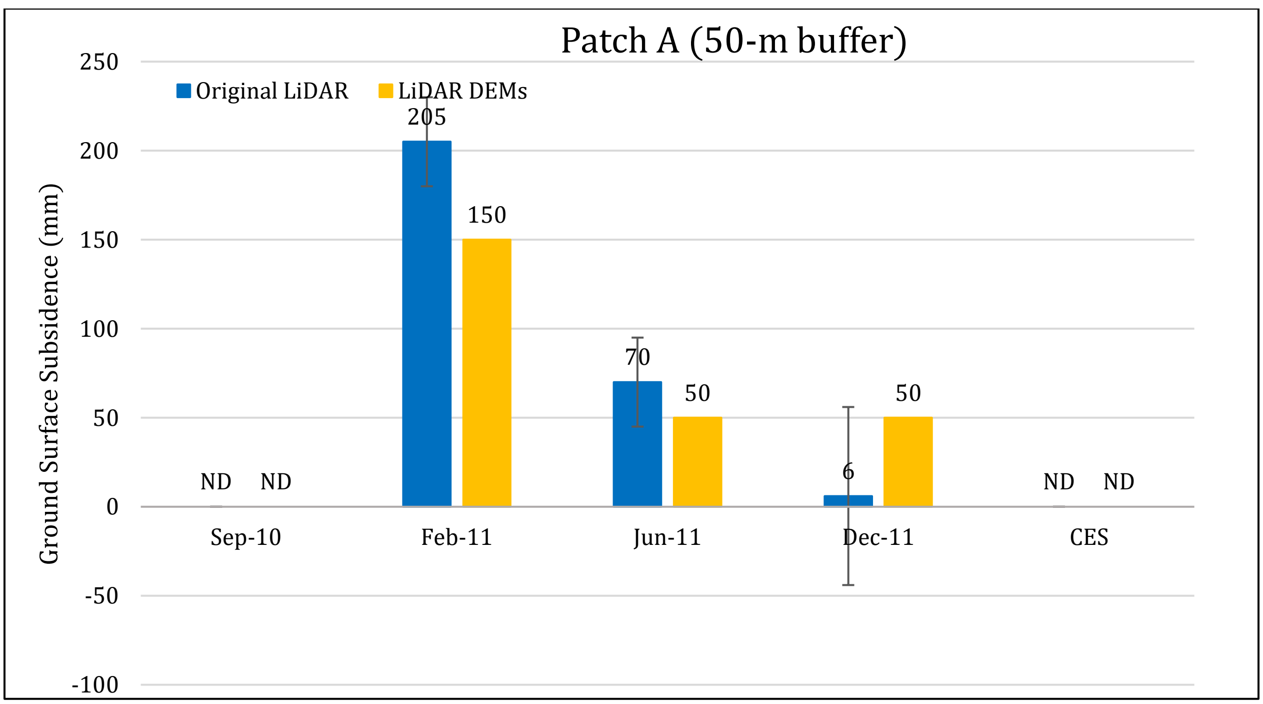

Figure 4: Comparison between ground surface subsidence determined from original LiDAR survey points and ground surface subsidence (50th %ile) estimated using LiDAR DEMs for Patch A (50-m buffer).

Note 2: The ground surface subsidence values determined from original LiDAR survey points are generally in agreement with the ground surface subsidence values estimated using LiDAR DEMs for all earthquake events.

Table 8a: Ejecta-Induced settlement for the top 20 m of the soil profile for Patch A (10-m buffer) for the 50th %ile PGA, P_L=50%, and C_{FC}=0.13 using BI-2014, ZRB-2002, and I_C cutoff of 2.6.

Earthquake Event(s)	M_W	PGA (g)	Depth to Groundwater (m)	S_T (mm)	S_{V1D} (mm)	$S_{E,L}$ (mm)
Sep-10	7.1	0.18	2.5	ND	29±20	ND
Feb-11	6.2	0.43	2.5	234±25	95±50	139±56
Jun-11	6.2	0.22	2.5	76±25	36±25	40±35
Dec-11	6.1	0.35	1.5	26±50	94±50	-68±71

Notes: S_T = Total settlement (Table 6); S_{V1D} = Average vertical settlement due to volumetric compression using Boulanger and Idriss (2014) (BI-2014), Zhang et al. (2002) (ZRB-2002) procedures and de Greef and Lengkeek (2018) thin-layer correction; $S_{E,L}$ = Ejecta-induced settlement as the difference between the LiDAR-based S_T and S_{V1D}; ND = Not determined due to the anthropogenic changes prior to the Sep 2010 LiDAR survey.

Table 8b: Ejecta-Induced settlement for the top 20 m of the soil profile for Patch A (20-m buffer) for the 50th %ile PGA, P_L=50%, and C_{FC}=0.13 using BI-2014, ZRB-2002, and I_C cutoff of 2.6.

Earthquake Event(s)	M_W	PGA (g)	Depth to Groundwater (m)	S_T (mm)	S_{V1D} (mm)	$S_{E,L}$ (mm)
Sep-10	7.1	0.18	2.5	ND	29±20	ND
Feb-11	6.2	0.43	2.5	218±25	95±50	123±56
Jun-11	6.2	0.22	2.5	73±25	36±25	37±35
Dec-11	6.1	0.35	1.5	18±50	94±50	-77±71

Notes: S_T = Total settlement (Table 6); S_{V1D} = Average vertical settlement due to volumetric compression using Boulanger and Idriss (2014) (BI-2014), Zhang et al. (2002) (ZRB-2002) procedures and de Greef and Lengkeek (2018) thin-layer correction; $S_{E,L}$ = Ejecta-induced settlement as the difference between the LiDAR-based S_T and S_{V1D}; ND = Not determined due to the anthropogenic changes prior to the Sep 2010 LiDAR survey.

Table 8c: Ejecta-Induced settlement for the top 20 m of the soil profile for Patch A (50-m buffer) for the 50th %ile PGA, P_L=50%, and C_{FC}=0.13 using BI-2014, ZRB-2002, and I_C cutoff of 2.6.

Earthquake Event(s)	M_W	PGA (g)	Depth to Groundwater (m)	S_T (mm)	S_{V1D} (mm)	$S_{E,L}$ (mm)
Sep-10	7.1	0.18	2.5	ND	20±20	ND
Feb-11	6.2	0.43	2.5	205±25	94±50	111±56
Jun-11	6.2	0.22	2.5	70±25	26±25	44±35
Dec-11	6.1	0.35	1.5	6±50	82±50	-76±71

Notes: S_T = Total settlement (Table 6); S_{V1D} = Average vertical settlement due to volumetric compression using Boulanger and Idriss (2014) (BI-2014), Zhang et al. (2002) (ZRB-2002) procedures and de Greef and Lengkeek (2018) thin-layer correction; $S_{E,L}$ = Ejecta-induced settlement as the difference between the LiDAR-based S_T and S_{V1D}; ND = Not determined due to the anthropogenic changes prior to the Sep 2010 LiDAR survey.

Note 3: The uncertainty for volumetric settlement was derived based on the sensitivity of volumetric settlement to PGA, C_{FC}, and P_L for each earthquake event for VsVp 57203 *Shirley Intermediate School* and CC LIQ 1 – CPT 5586 – *Vivian St* sites. Taking the 50th percentile as the baseline case, the minimum and maximum values corresponding to the difference between the 25th percentile and the 50th percentile and the 75th percentile and the 50th percentile were determined. The arithmetic mean of the range of the minimum and maximum difference was evaluated for each patch at the two sites. The maximum arithmetic mean for each earthquake event was rounded to the nearest five and used as the uncertainty value. Accordingly, the 1-D volumetric settlement uncertainties of ±20, ±50, ±25, and ±50 mm for the Sep-10, Feb-11, Jun-11, and Dec-11 earthquake events, respectively, were used for all sites in this study.

Table 9a: Coverage area and height of ejecta estimates for Patch A (10-m buffer) using photographs.

EQ Event	$H_{E,thick1}$ (mm)	$A_{E,thick1}$ (m^2)	$H_{E,thick2}$ (mm)	$A_{E,thick2}$ (m^2)	$H_{E,thin1}$ (mm)	$A_{E,thin1}$ (m^2)	$H_{E,thin2}$ (mm)	$A_{E,thin2}$ (m^2)	A_T (m^2)
Sep-10	0	0	0	0	0	0	0	0	314
Feb-11	100-160	33.9	0	0	0	0	10-20	249	314
Jun-11	0	0	60-100	1.1	0	0	10-20	111	314
Dec-11	0	0	0	0	10-30	33.0	3-6	76.2	314

Notes: $A_{E,thin/thick}$ = Coverage area of thin/thick ejecta layers; $H_{E, thin/thick}$ = Lower-upper estimate of height of thin/thick ejecta layers; A_T= Total assessment area of a buffer being considered.

Table 9b: Coverage area and height of ejecta estimates for Patch A (20-m buffer) using photographs.

EQ Event	$H_{E,thick1}$ (mm)	$A_{E,thick1}$ (m²)	$H_{E,thick2}$ (mm)	$A_{E,thick2}$ (m²)	$H_{E,thin1}$ (mm)	$A_{E,thin1}$ (m²)	$H_{E,thin2}$ (mm)	$A_{E,thin2}$ (m²)	A_T (m²)
Sep-10	0	0	0	0	0	0	0	0	1257
Feb-11	100-160	41.5	0	0	40-60	8.8	10-20	590	1257
Jun-11	0	0	60-100	36.4	0	0	10-20	292	1257
Dec-11	70-140	17.7	40-70	9.3	10-30	133	3-6	117	1257

Notes: $A_{E,thin/thick}$ = Coverage area of thin/thick ejecta layers; $H_{E, thin/thick}$ = Lower-upper estimate of height of thin/thick ejecta layers; A_T= Total assessment area of a buffer being considered.

Table 9c: Coverage area and height of ejecta estimates for Patch A (50-m buffer) using photographs.

EQ Event	$H_{E,thick1}$ (mm)	$A_{E,thick1}$ (m²)	$H_{E,thick2}$ (mm)	$A_{E,thick2}$ (m²)	$H_{E,thin1}$ (mm)	$A_{E,thin1}$ (m²)	$H_{E,thin2}$ (mm)	$A_{E,thin2}$ (m²)	A_T (m²)
Sep-10	0	0	0	0	0	0	0	0	7107
Feb-11	100-160	169	60-100	163	40-60	78.5	10-20	2475	7107
Jun-11	0	0	60-100	187	30-60	122	10-20	1128	7283
Dec-11	70-140	105	40-70	75	10-30	688	3-6	217	7107

Notes: $A_{E,thin/thick}$ = Coverage area of thin/thick ejecta layers; $H_{E, thin/thick}$ = Lower-upper estimate of height of thin/thick ejecta layers; A_T= Total assessment area of a buffer being considered.

Note 4: The values in Table 9 correspond to the coverage area of ejecta outlined in aerial photographs (Figures 12, 13, 20, and 61-64) and the lower and upper estimates of ejecta height based on geometrical approximations. The ejecta-induced settlement using photographs and engineering judgment, $S_{E,P}$, is estimated as

$$S_{E,P} = \frac{\sum_{i=1}^{a} A_{E,thick,i} * H_{E,thick,i} + \sum_{j=1}^{b} A_{E,thin,j} * H_{E,thin,j}}{A_T} = \frac{\sum_{i=1}^{a} V_{E,thick,i} + \sum_{j=1}^{b} V_{E,thin,j}}{A_T}$$

where

- $A_{E,thick,i}$ and $H_{E,thick,i}$ are the area and the height, respectively, of a thick ejecta layer;
- $A_{E,thin,j}$ and $H_{E,thin,j}$ are the area and the height, respectively, of a thin ejecta layer;
- A_T is the total assessment area for a buffer being considered (Figure 1).

Table 10: Ejecta-induced settlement estimates for Patch A based on photographs.

Earthquake Event	Patch A (10-m buffer)		Patch A (20-m buffer)		Patch A (50-m buffer)	
	$S_{E,P,lower}$ (mm)	$S_{E,P,upper}$ (mm)	$S_{E,P,lower}$ (mm)	$S_{E,P,upper}$ (mm)	$S_{E,P,lower}$ (mm)	$S_{E,P,upper}$ (mm)
Sep-10	0	0	0	0	0	0
Feb-11	19	33	8	15	8	14
Jun-11	4	7	4	8	4	7
Dec-11	2	5	3	6	3	6

Note: $S_{E,P,lower}$ and $S_{E,P,upper}$ correspond to lower and upper estimates of $S_{E,P}$, respectively.

Table 11: Best final estimates of ejecta-induced settlement for Patch A.

EQ Event	Patch A (10-m buffer)			Patch A (20-m buffer)			Patch A (50-m buffer)		
	$S_{E,L}$ (mm)	$S_{E,P}$ (mm)	$S_{E,final}$ (mm)	$S_{E,L}$ (mm)	$S_{E,P}$ (mm)	$S_{E,final}$ (mm)	$S_{E,L}$ (mm)	$S_{E,P}$ (mm)	$S_{E,final}$ (mm)
Sep-10	ND	0	0	ND	0	0	ND	0	0
Feb-11	139±56	26±7	35±10	123±56	11.5±3.5	25±5	111±56	11±3	20±5
Jun-11	40±35	5.5±1.5	10±5	37±35	6±2	10±5	44±35	5.5±1.5	10±5
Dec-11	-68±71	3.5±1.5	5±5	-77±71	4.5±1.5	5±5	-76±71	4.5±1.5	5±5

Notes: $S_{E,L}$ = Ejecta-induced settlement based on LiDAR data reported in Table 8; $S_{E,P}$ = Median ejecta-induced settlement for the range of values reported in Table 10; $S_{E,final}$ = Best final estimate of ejecta-induced settlement rounded to the nearest 5; Final plus/minus values are also rounded to the nearest 5; ND = Not determined.

Note 5:

- Patch A: $S_{E,final}$ is based solely on $S_{E,P}$ for the Sep-10 and Dec-11 EQs due to the evident absence of ejecta for the Sep-10 EQ and the negative $S_{E,L}$ values for the Dec-11 EQ. $S_{E,final}$ for the Feb-11 and Jun-11 EQs is a weighted average of $S_{E,L}$ and $S_{E,P}$ with weights of 0.1 and 0.9, respectively. The uncertainty associated with $S_{E,final}$ is also a weighted average of uncertainties associated with $S_{E,L}$ and $S_{E,P}$ with the same respective weights of 0.1 and 0.9.
- The weight coefficients are based on the LiDAR error bands, LPI prediction error (Maurer et al. 2014[3]), presence of ejecta at the time of LiDAR surveys, and completeness of visual evidence (i.e., ground and aerial photographs and EQC LDAT property inspection reports for the site), and discrepancy between the LiDAR-based ejecta-induced settlement estimates and the observed ejecta quantum. The Mark Treffers Dr site is not in the apparent zone of higher/lower ground surface subsidence for the Sep-10/Feb-11 EQ. The site is in the zone of correct LPI prediction of liquefaction severity for the Sep-10 EQ and slight LPI overprediction of liquefaction severity for the Feb-11 EQ. The LDAT property inspection reports and ground photographs are not available.

Summary 1:

The best estimate of the ejecta-induced free-field ground settlement at the Mark Treffers Dr site for the SEP 2010, FEB 2011, JUN 2011, and DEC 2011 earthquake is 0 mm, 35±10 mm, 10±5 mm, and 5±5 mm, respectively.

[3] Maurer, B. W., Green, R. A., Cubrinovski, M., & Bradley, B. A. (2014). Evaluation of the Liquefaction Potential Index for Assessing Liquefaction Hazard in Christchurch, New Zealand. *Journal of Geotechnical and Geoenvironmental Engineering*, 140(7), 04014032-1-11. doi:10.1061/(asce)gt.1943-5606.0001117

Figure 5: Location of the site.

Figure 6: Position of the site relative to nearby buildings, vegetation, and free-face features.

Figure 7: Street view of the flat land.

Figure 8: Satellite image of the site taken in Dec 2004.

Figure 9: Satellite image of the site taken in Apr 2005.

Figure 10: Satellite image of the site taken in Feb 2006.

Figure 11: Satellite image of the site taken in Mar 2009.

Figure 12: Satellite image of the site taken on Sep 3, 2010.

Figure 13: Satellite image of the site taken on Sep 5, 2010.

Figure 14: Satellite image of the site taken on Feb 7, 2011.

Figure 15: Satellite image of the site taken on Feb 23, 2011.

Figure 16: Satellite image of the site taken on Feb 26, 2011.

Figure 17: Satellite image of the site taken on Mar 8, 2011.

Figure 18: Satellite image of the site taken in Apr 2012.

Figure 19: Satellite image of the site taken in Nov 2011.

Figure 20: Aerial photograph of the site taken on Sep 4, 2010.

Figure 21: Aerial photograph of the site taken on Feb 24, 2011.

Figure 22: Aerial photograph of the site taken on June 14-15, 2011.

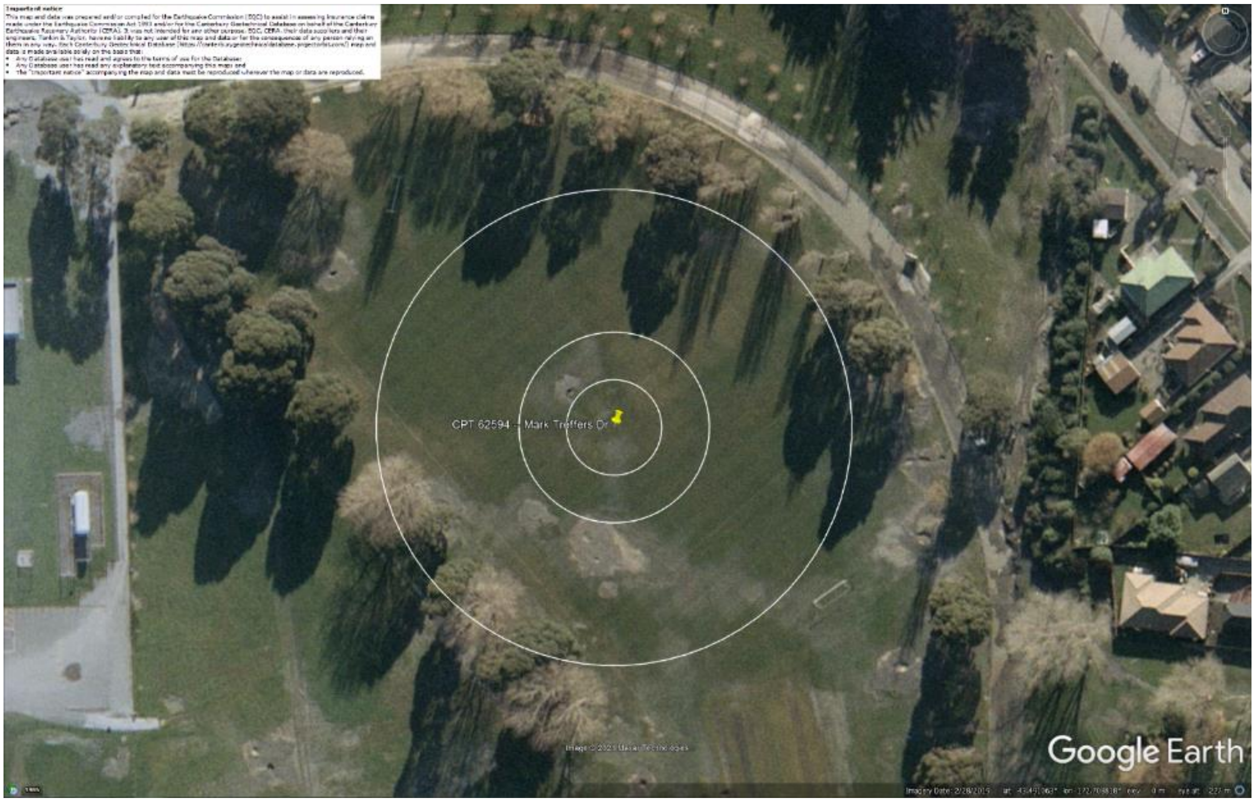

Figure 23: Aerial photograph of the site taken on June 16, 2011.

Figure 24: Aerial photograph of the site taken on Dec 24, 2011.

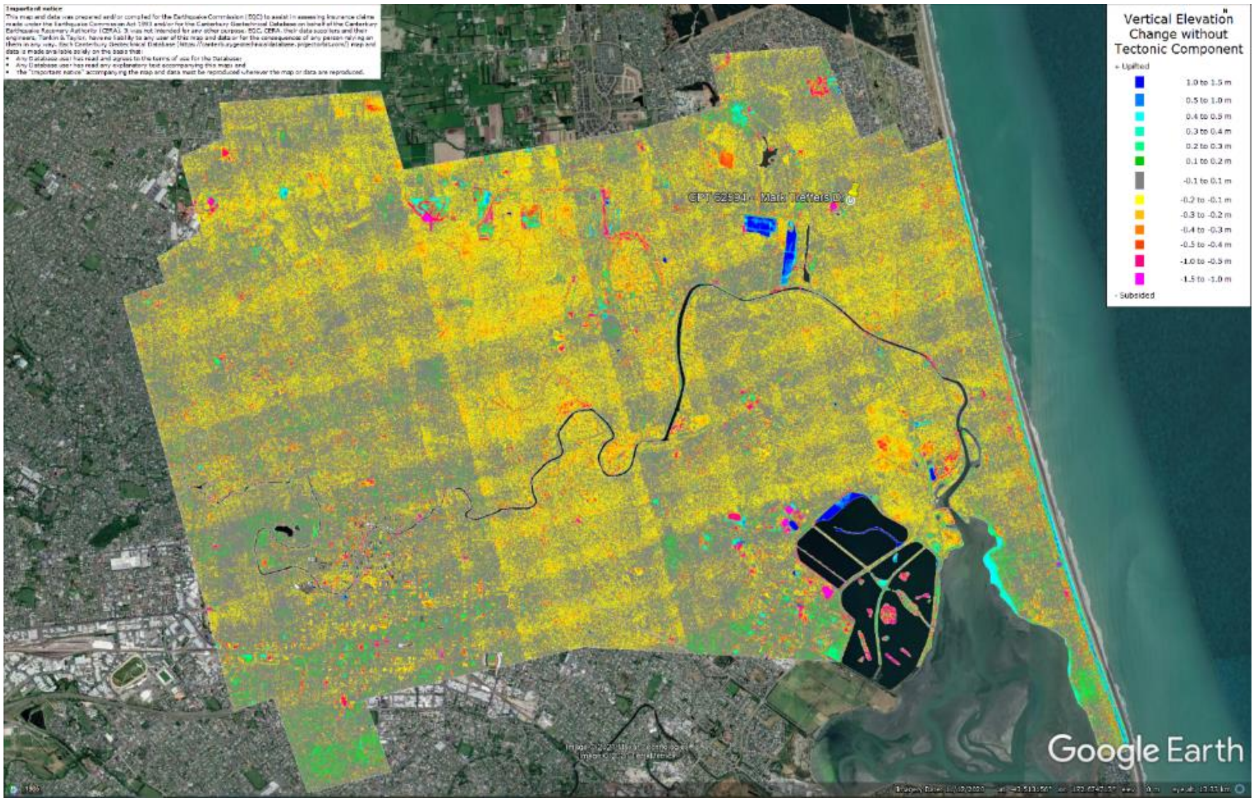

Figure 25: Vertical Ground Movements (Surface – Tectonic) for Sep 2010 Earthquake – the site is not in the apparent zone of overestimated/underestimated ground surface subsidence.

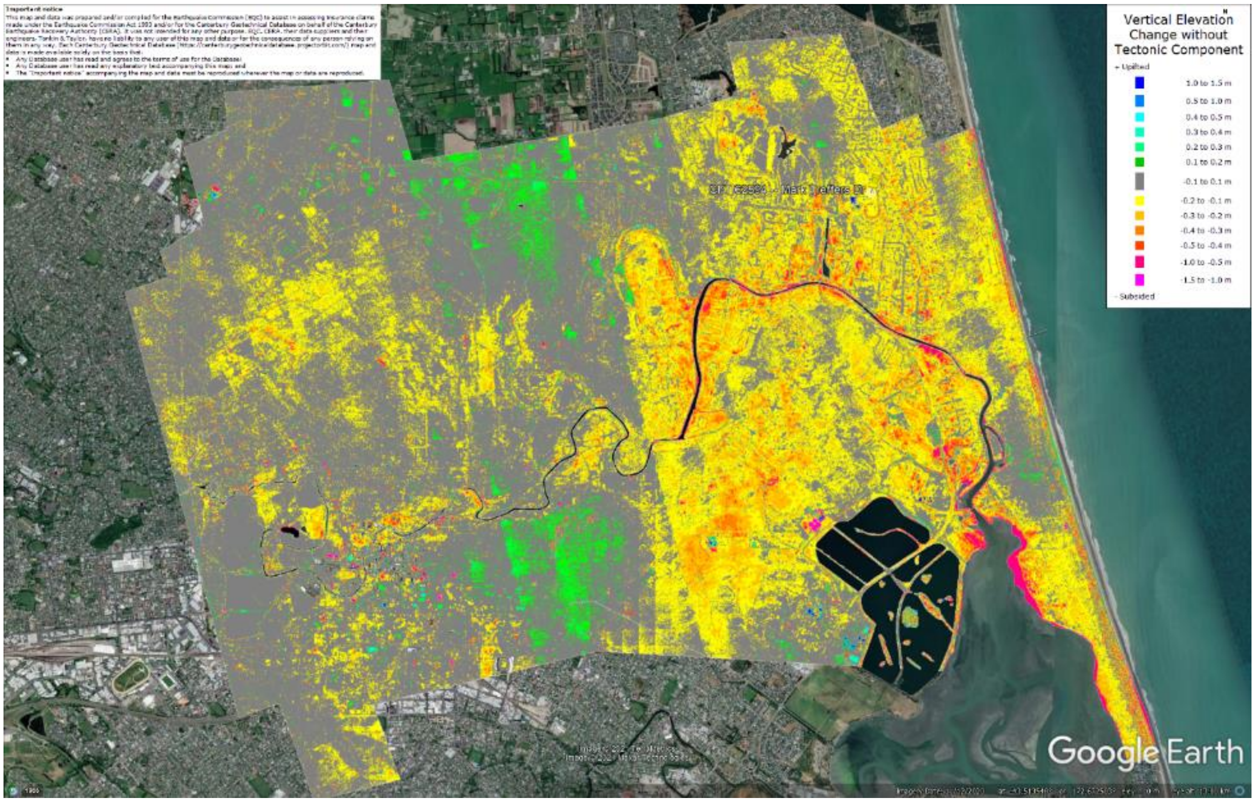

Figure 26: Vertical Ground Movements (Surface – Tectonic) for Feb 2011 Earthquake – the site is not in the apparent zone of overestimated/underestimated ground surface subsidence.

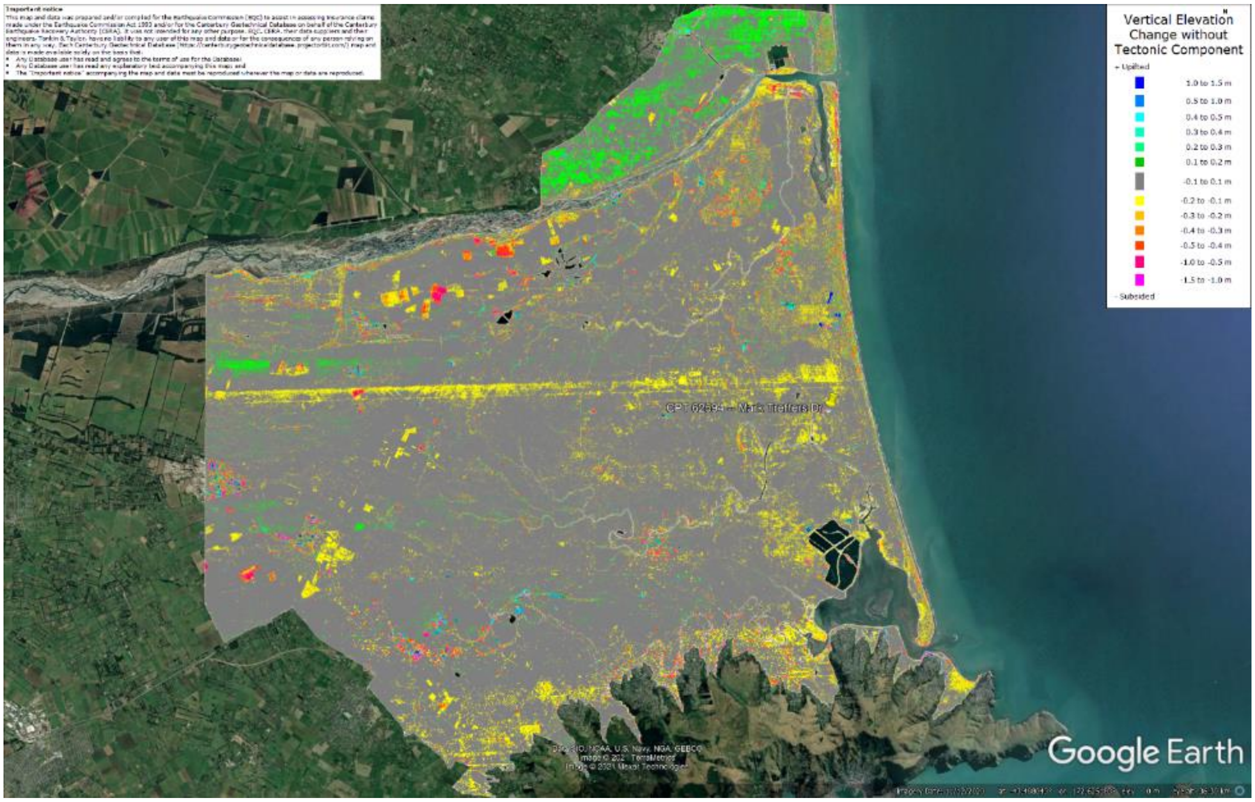

Figure 27: Vertical Ground Movements (Surface – Tectonic) for June 2011 Earthquake – the site is not in the apparent zone of overestimated/underestimated ground surface subsidence.

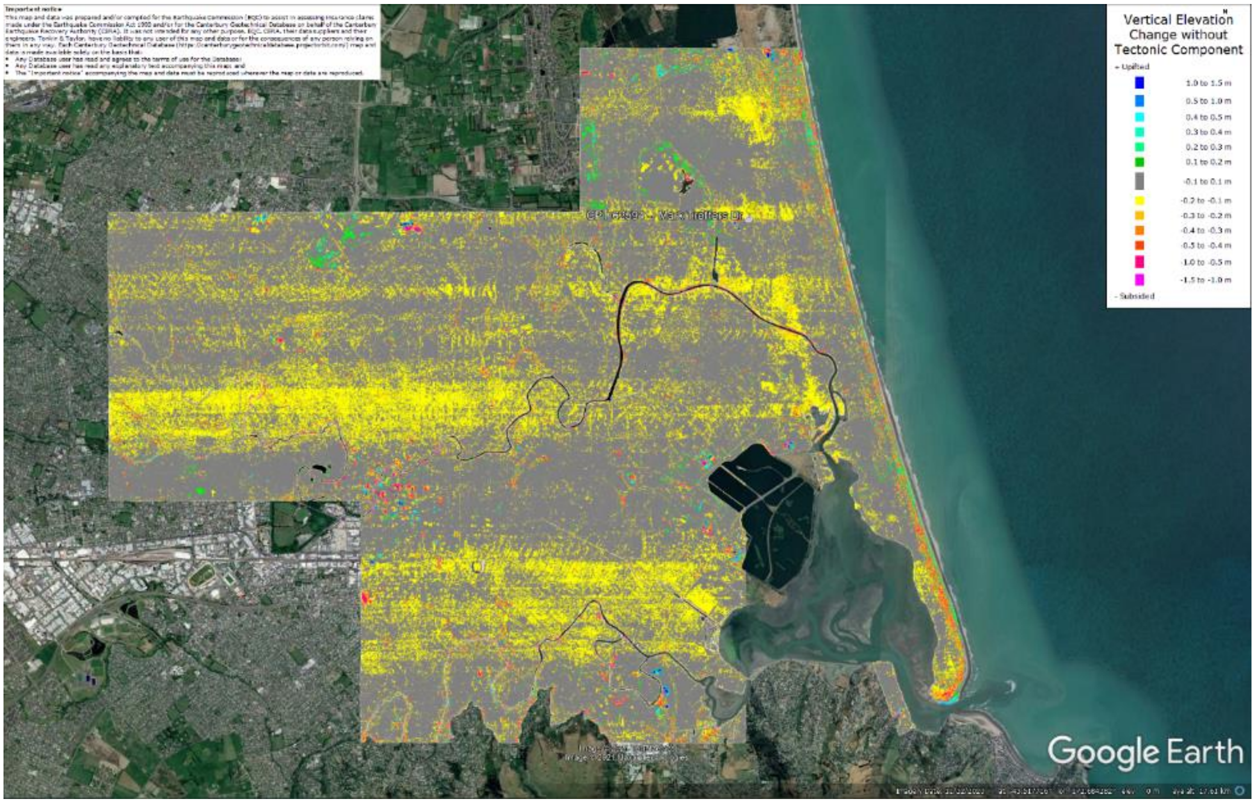

Figure 28: Vertical Ground Movements (Surface – Tectonic) for Dec 2011 Earthquake – the site is not in the apparent zone of overestimated/underestimated ground surface subsidence.

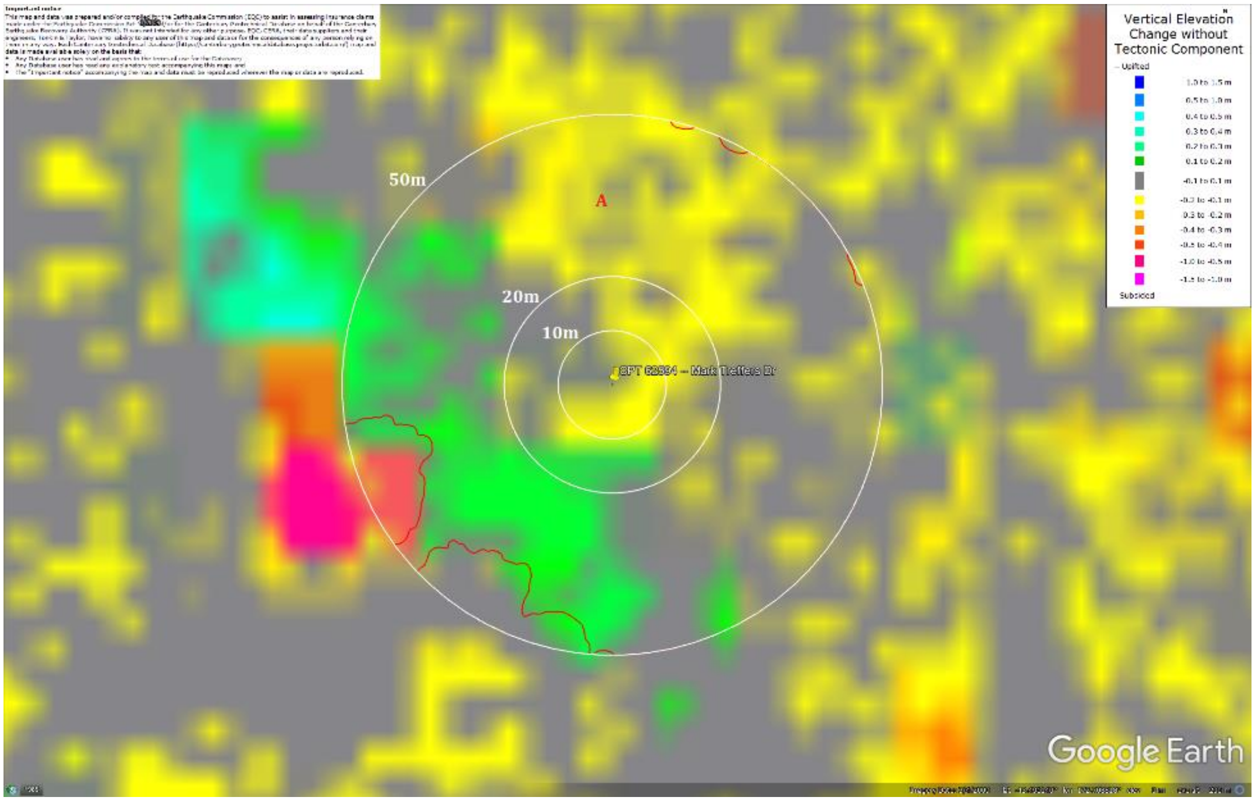

Figure 29: Ground surface subsidence without tectonic component for Sep 2010 Earthquake according to the LiDAR DEM.

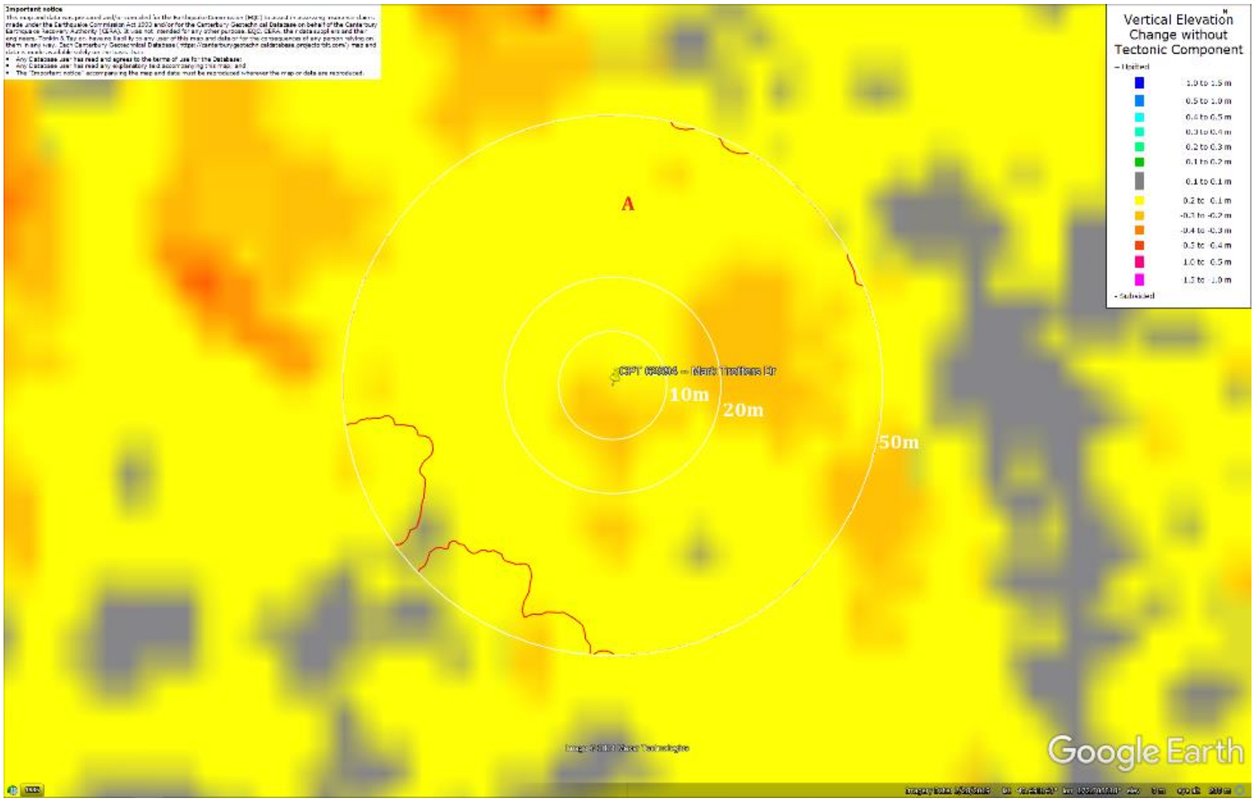

Figure 30: Ground surface subsidence without tectonic component for Feb 2011 Earthquake according to the LiDAR DEM.

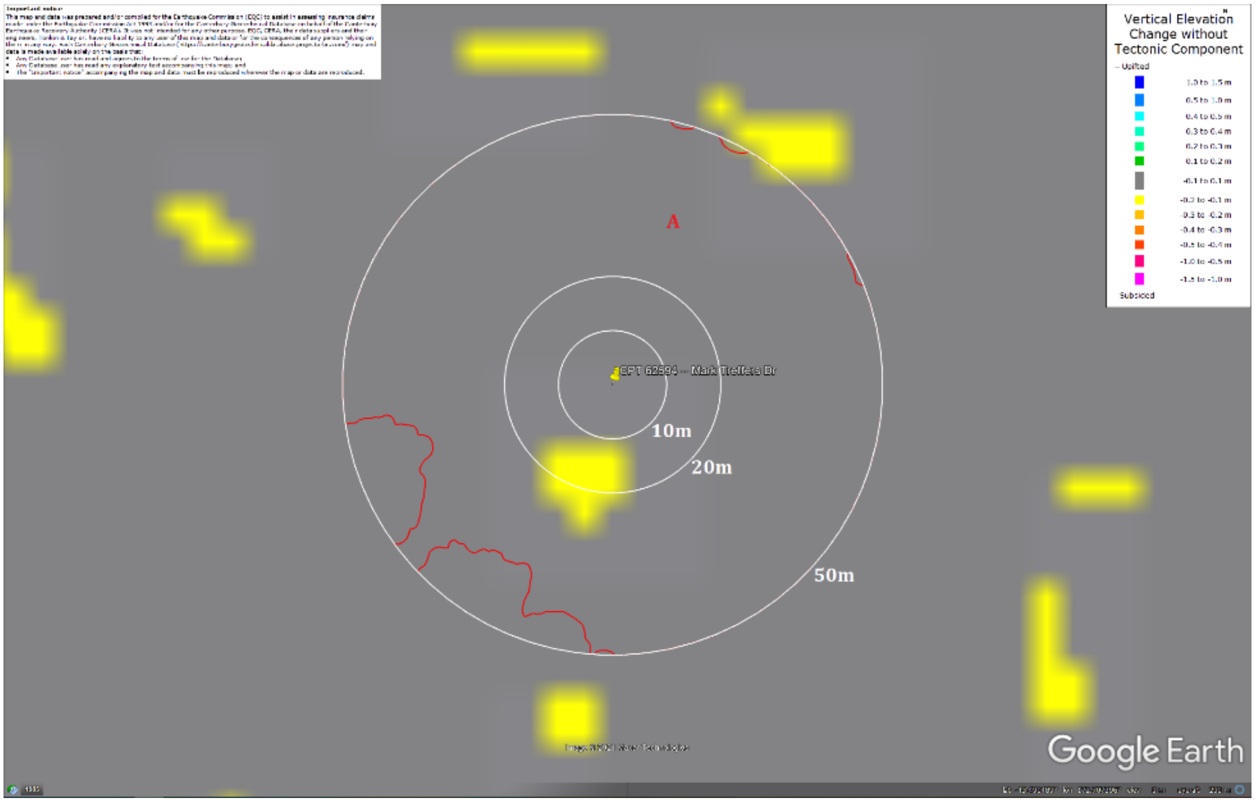

Figure 31: Ground surface subsidence without tectonic component for June 2011 Earthquake according to the LiDAR DEM.

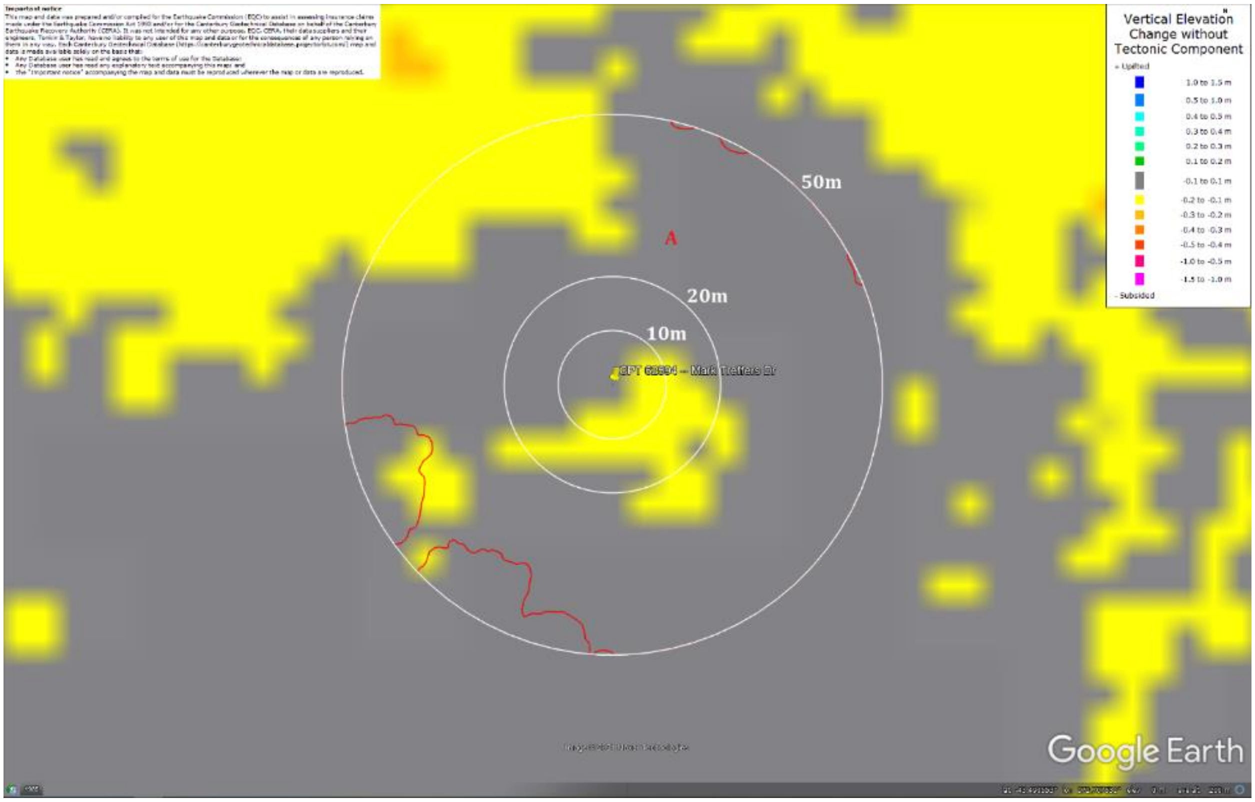

Figure 32: Ground surface subsidence without tectonic component for Dec 2011 Earthquake according to the LiDAR DEM.

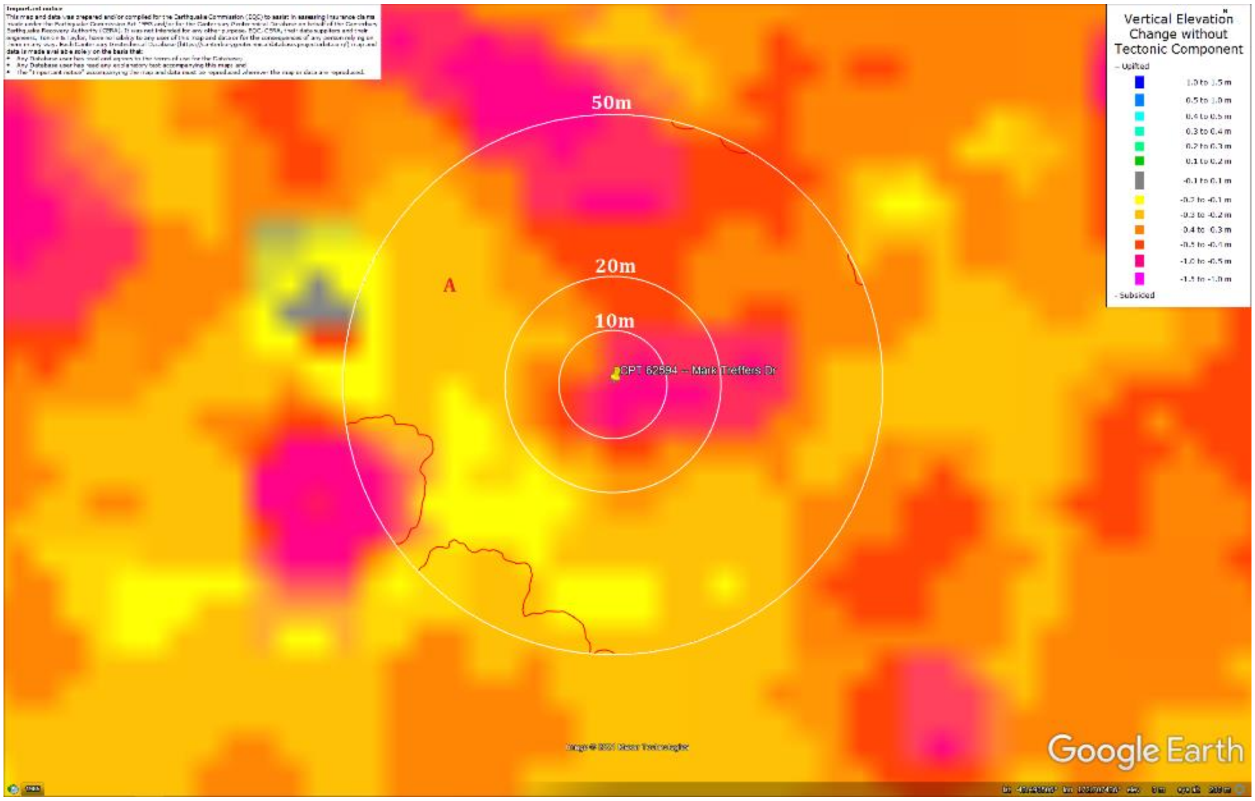

Figure 33: Ground surface subsidence without tectonic component for Canterbury Earthquake Sequence according to the LiDAR DEM.

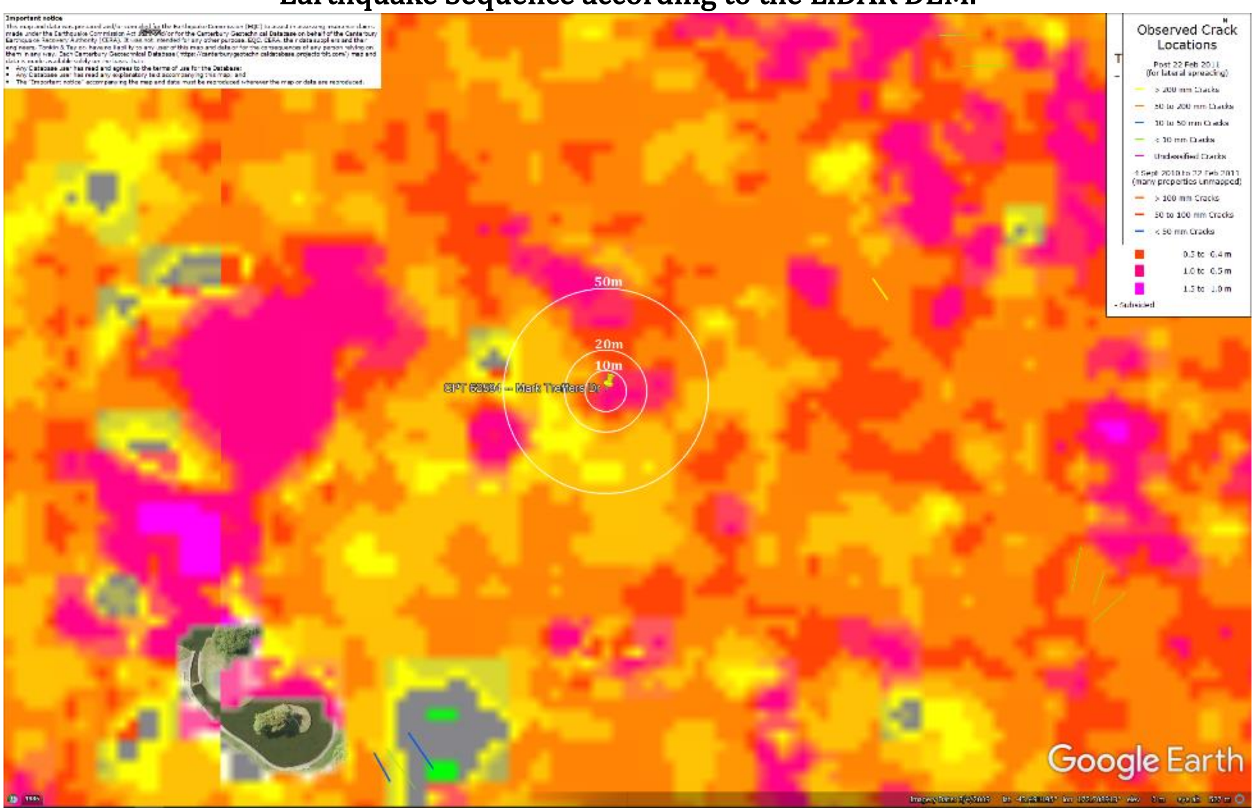

Figure 34: No lateral spreading for Canterbury Earthquake Sequence.

Figure 35: Vertical tectonic movements for Sep 2010 Earthquake.

Figure 36: Vertical tectonic movements for Feb 2011 Earthquake.

Figure 37: Vertical tectonic movements for June 2011 Earthquake.

Figure 38: Vertical tectonic movements for Dec 2011 Earthquake.

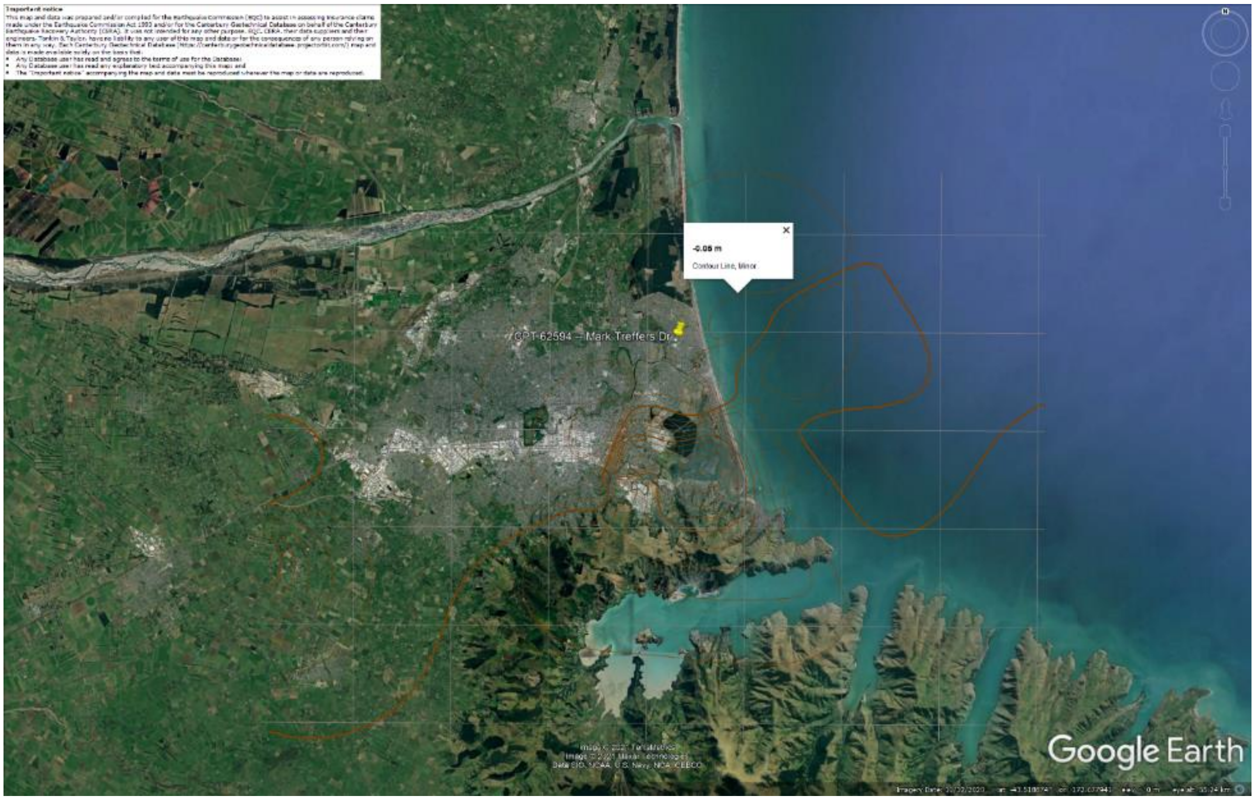

Figure 39: Vertical tectonic movements for Canterbury Earthquake Sequence.

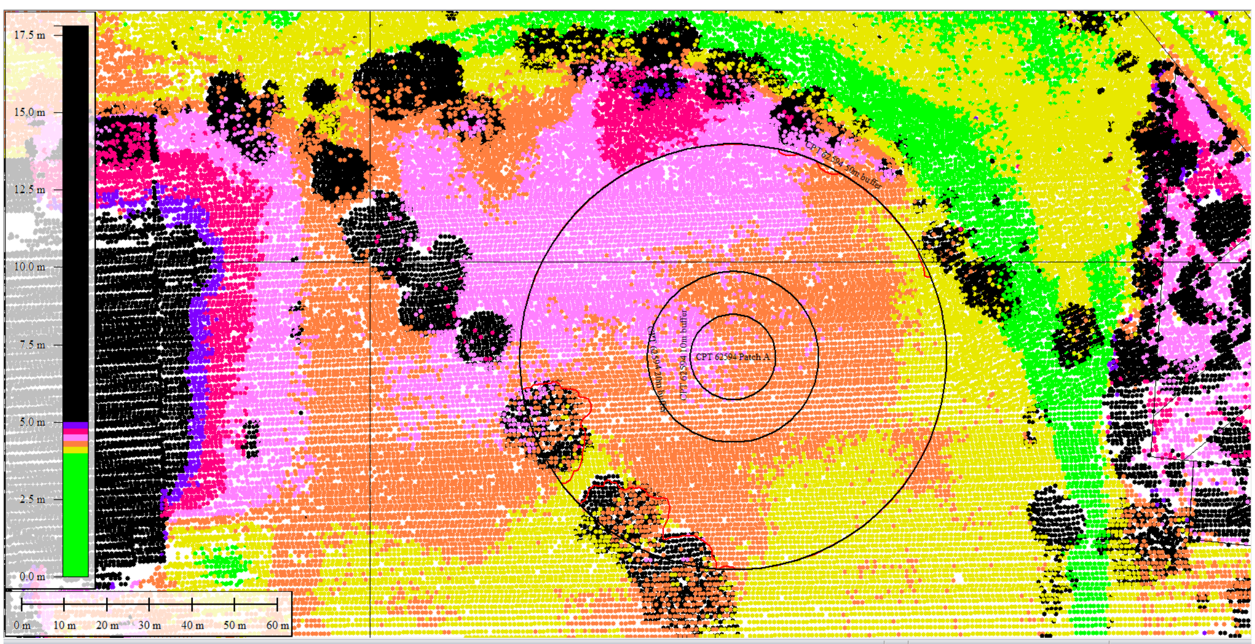

Figure 40: Sep 5, 2010 LiDAR survey.

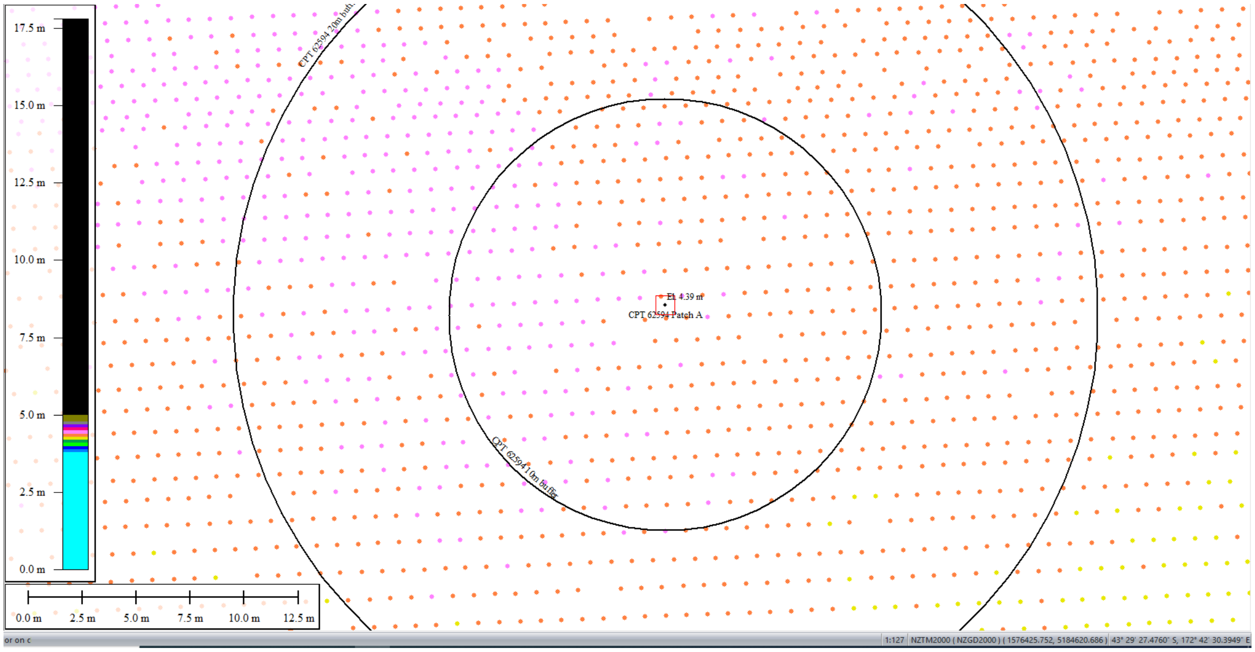

Figure 41: Ground surface elevation averaged over 10-m buffer for Patch A for Sep 5, 2010 LiDAR survey.

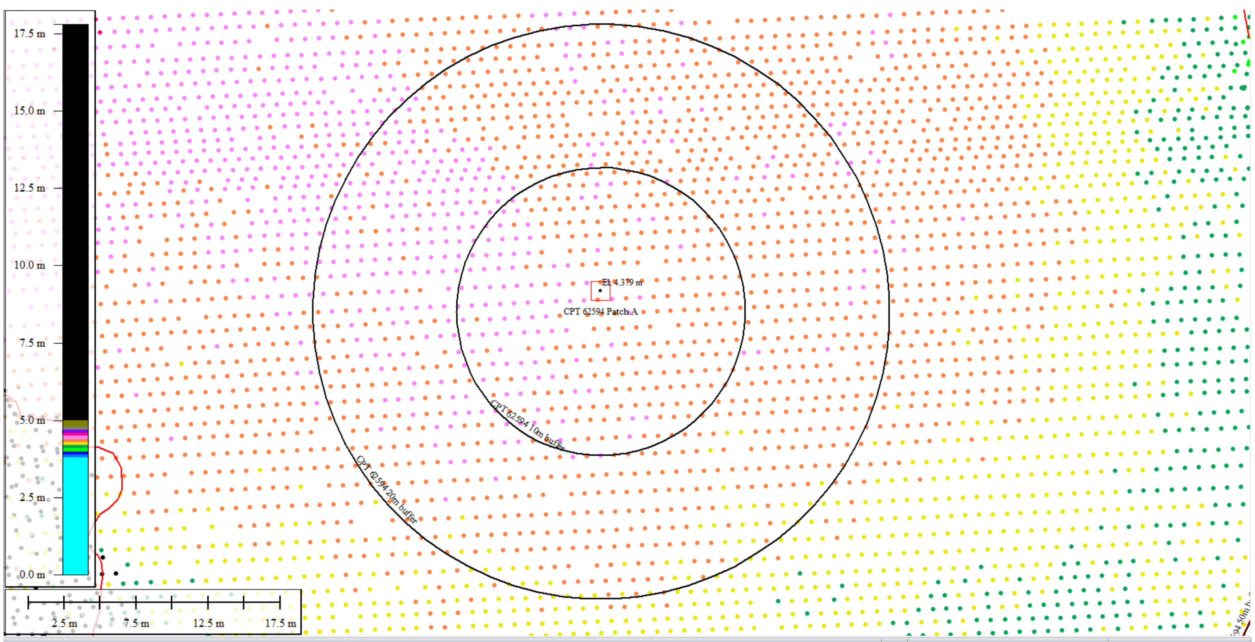

Figure 42: Ground surface elevation averaged over 20-m buffer for Patch A for Sep 5, 2010 LiDAR survey.

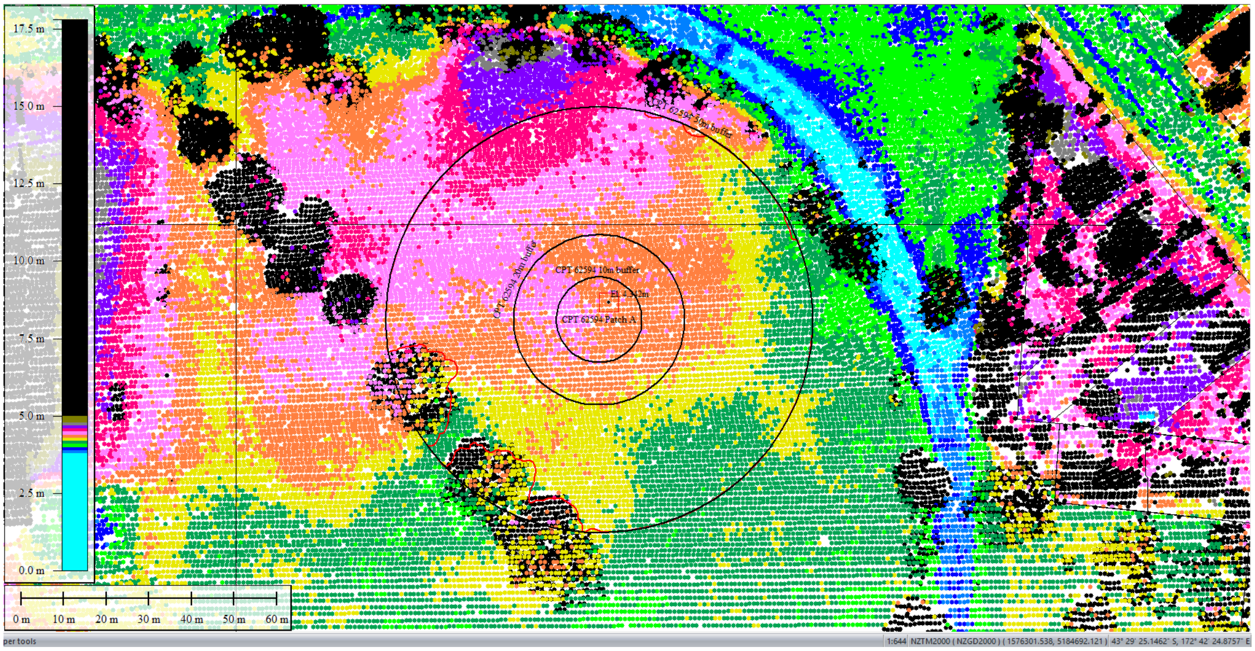

Figure 43: Ground surface elevation averaged over 50-m buffer for Patch A for Sep 5, 2010 LiDAR survey.

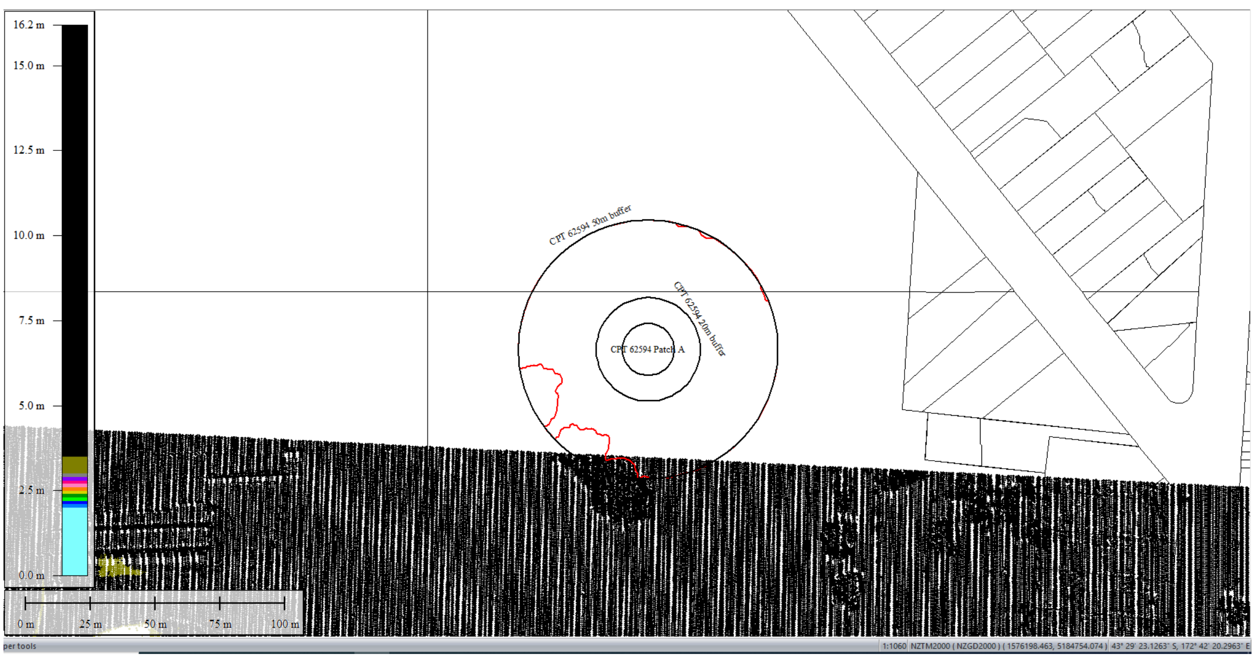

Figure 44: Mar 2011 LiDAR survey is not available.

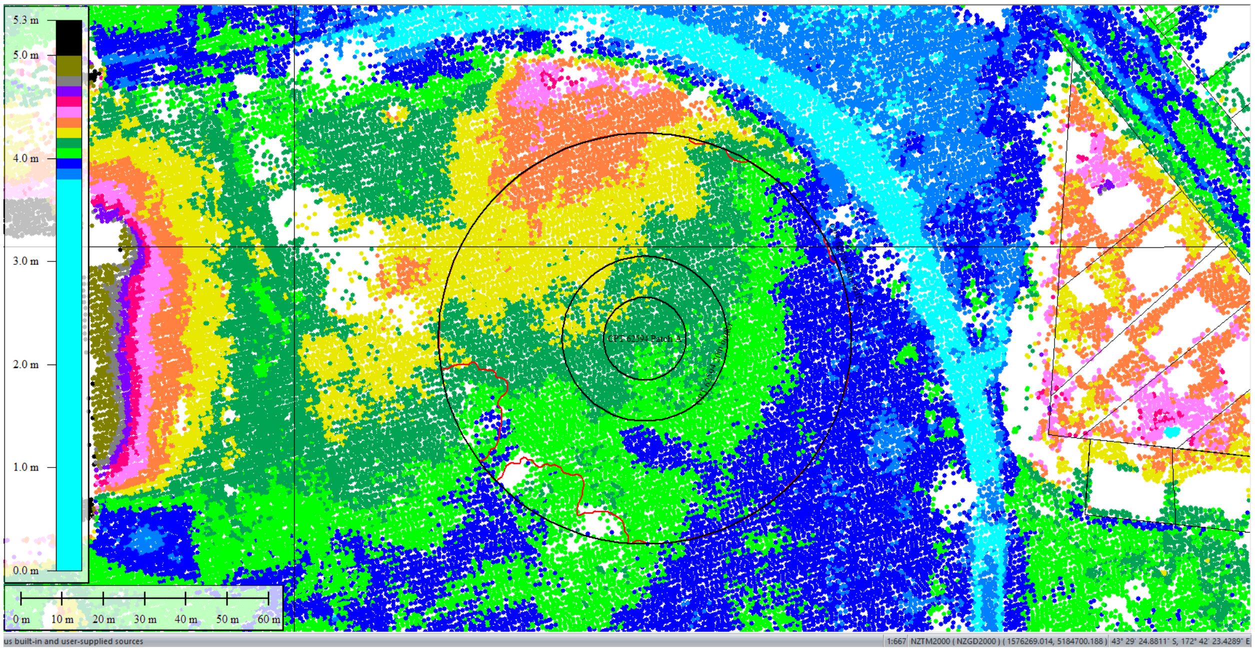

Figure 45: May 2011 LiDAR survey.

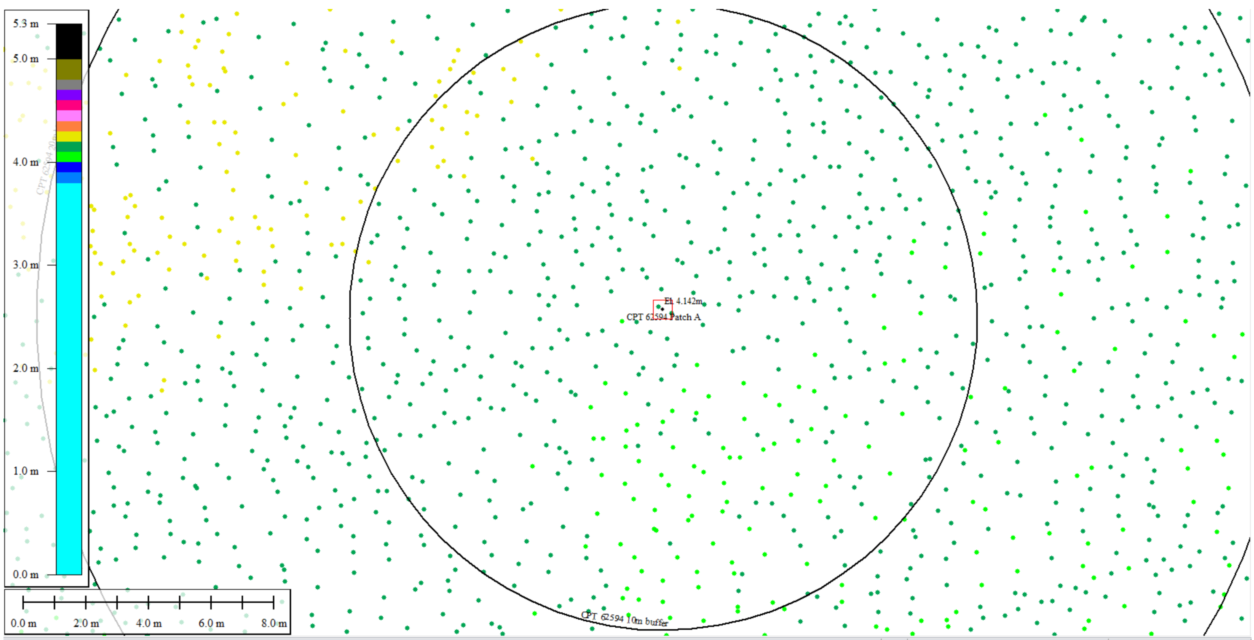

Figure 46: Ground surface elevation averaged over 10-m buffer for Patch A for May 2011 LiDAR survey.

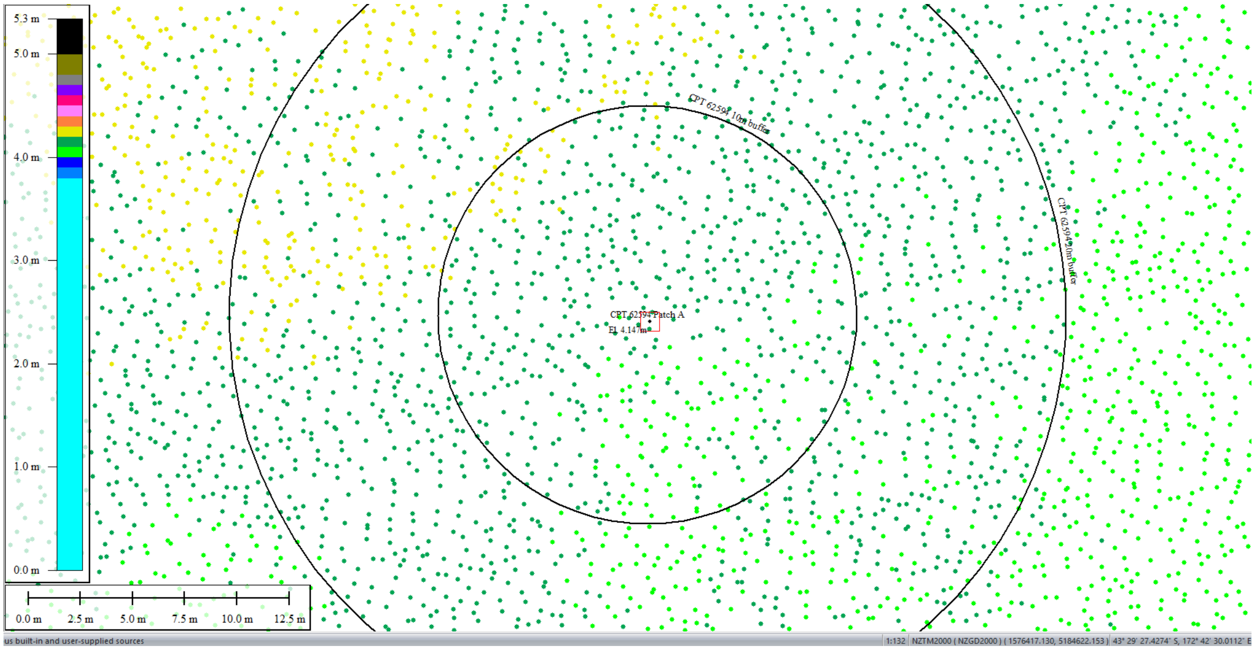

Figure 47: Ground surface elevation averaged over 20-m buffer for Patch A for May 2011 LiDAR survey.

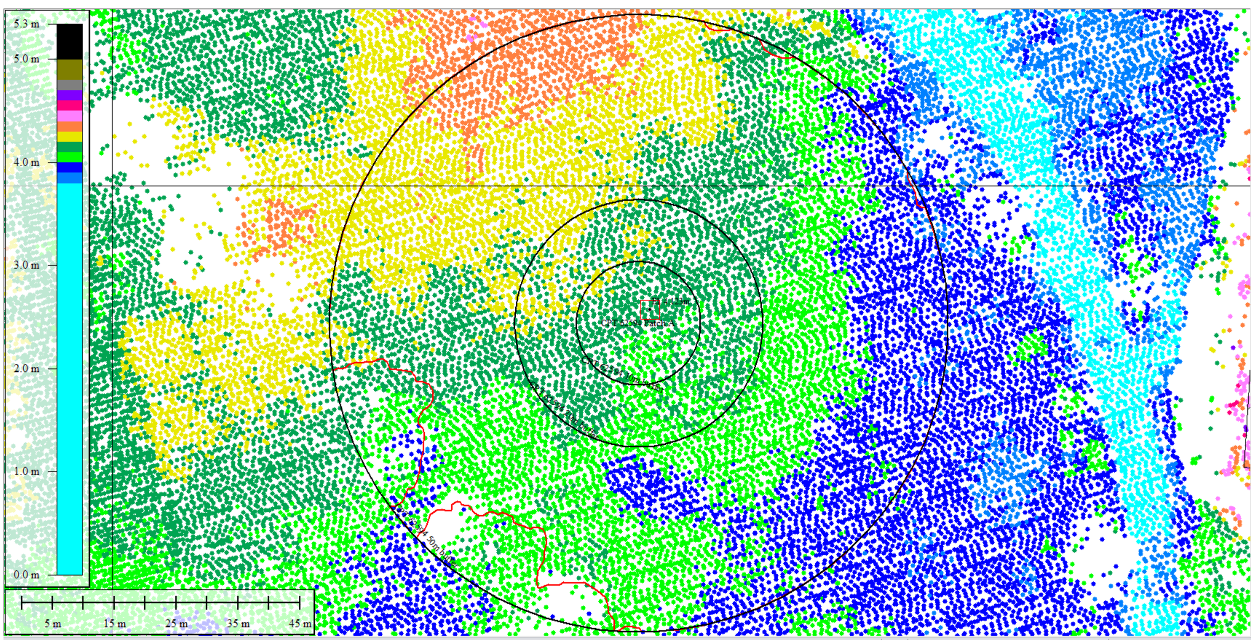

Figure 48: Ground surface elevation averaged over 50-m buffer for Patch A for May 2011 LiDAR survey.

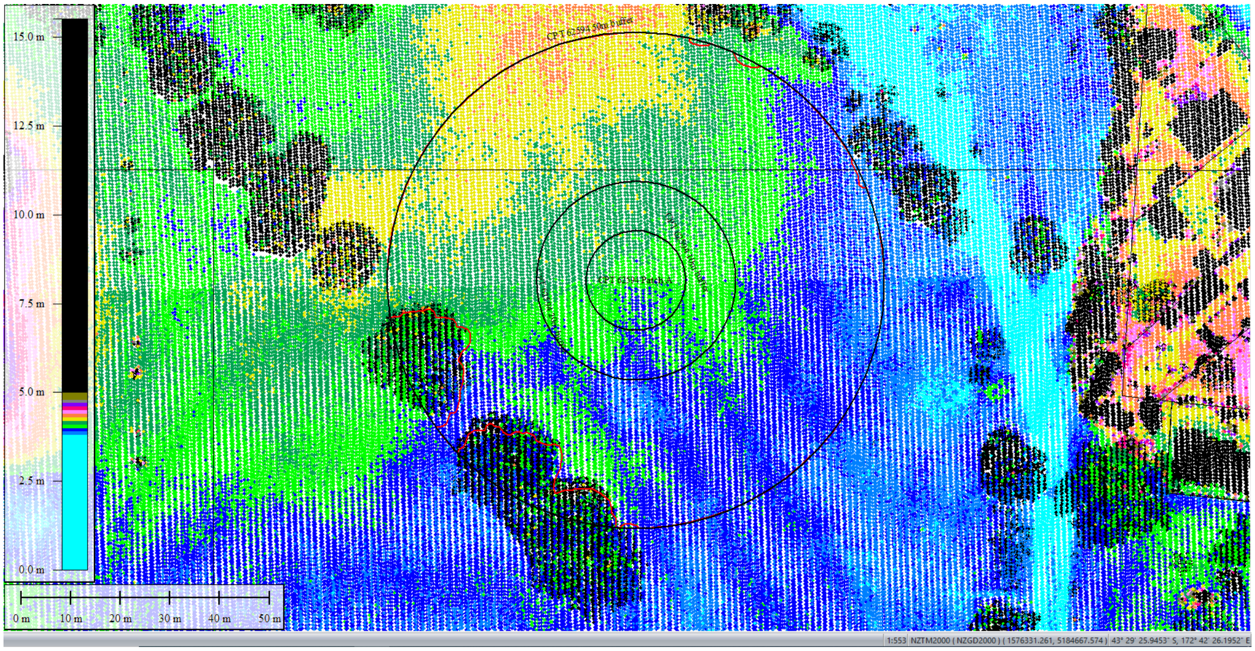

Figure 49: Sep 2011 LiDAR survey.

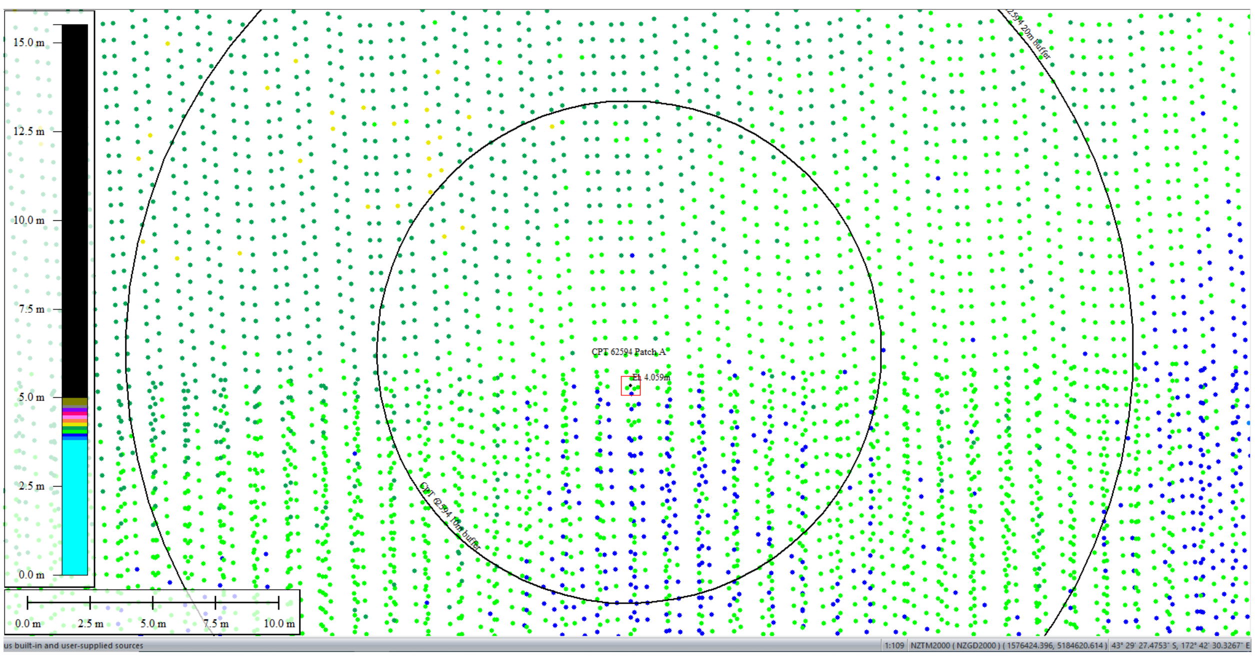

Figure 50: Ground surface elevation averaged over 10-m buffer for Patch A for Sep 2011 LiDAR survey.

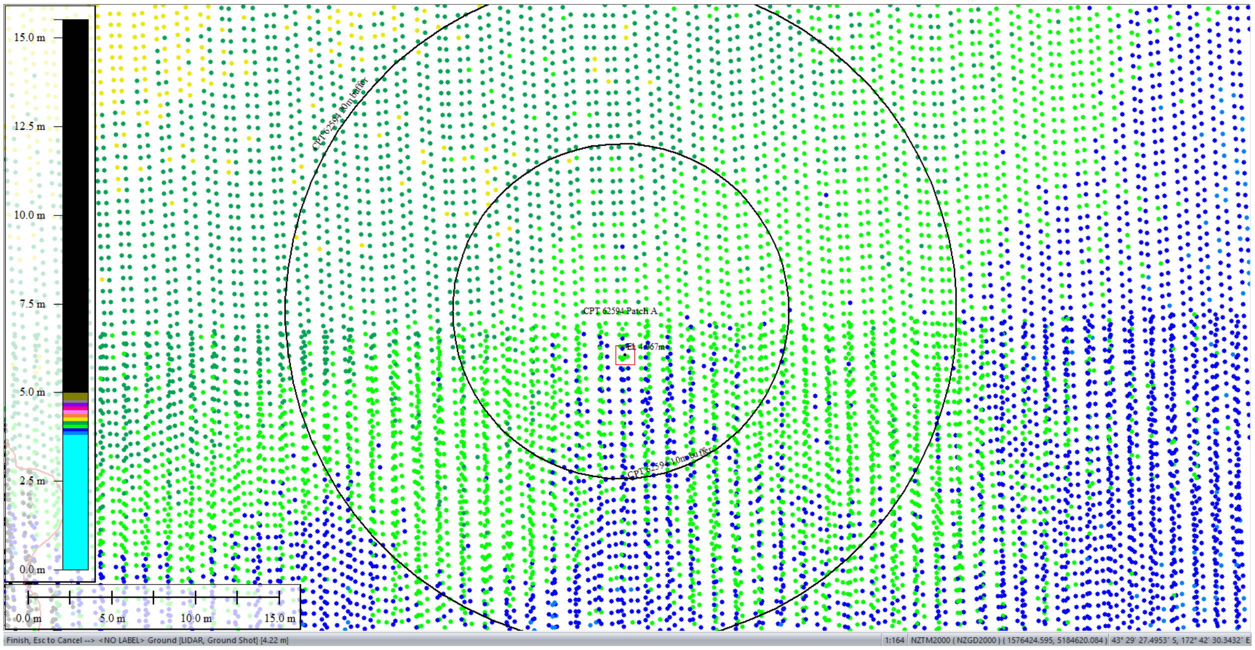

Figure 51: Ground surface elevation averaged over 20-m buffer for Patch A for Sep 2011 LiDAR survey.

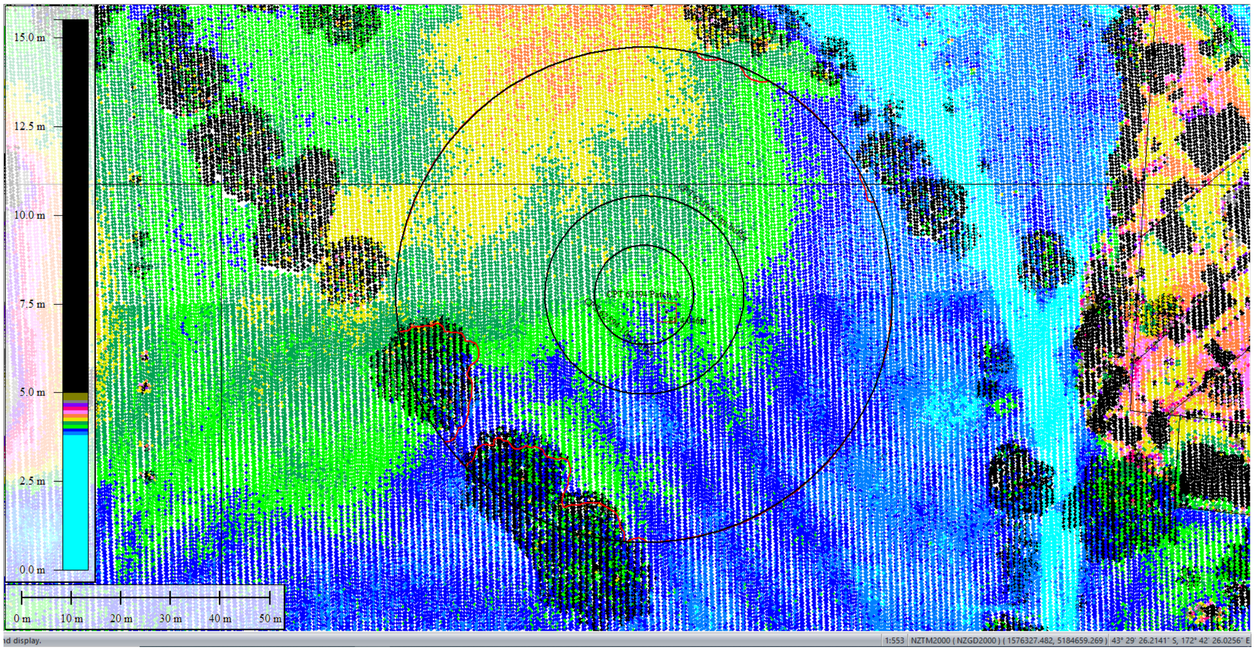

Figure 52: Ground surface elevation averaged over 50-m buffer for Patch A for Sep 2011 LiDAR survey.

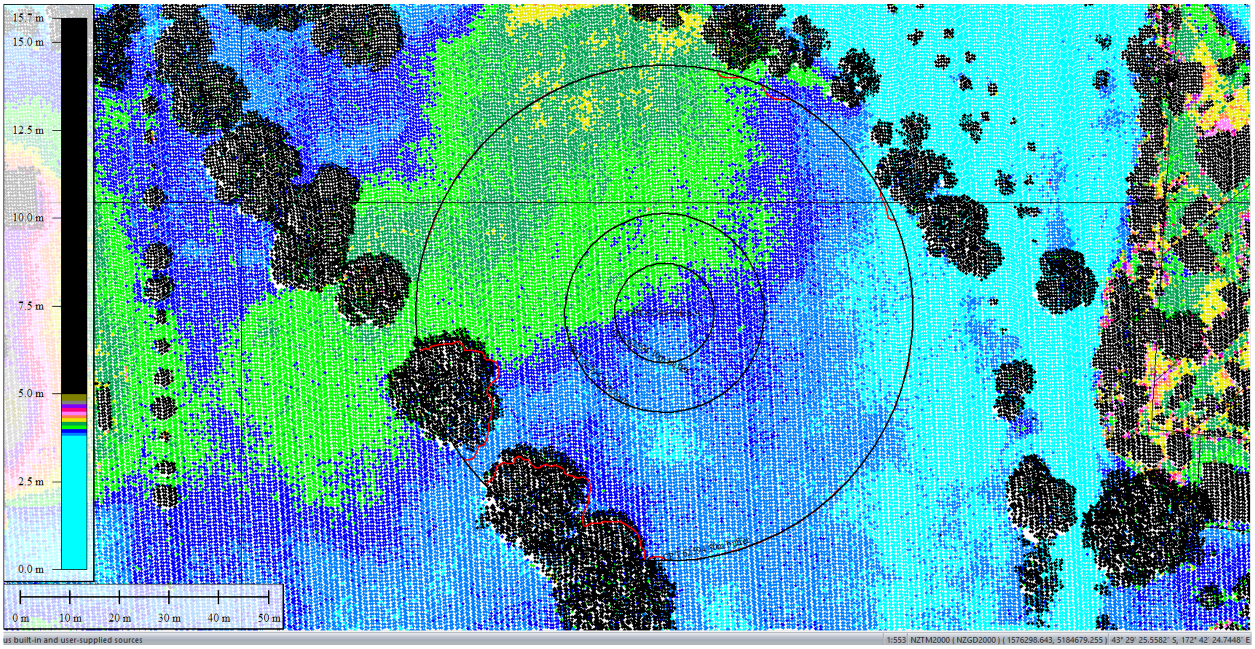

Figure 53: Feb 2012 LiDAR survey.

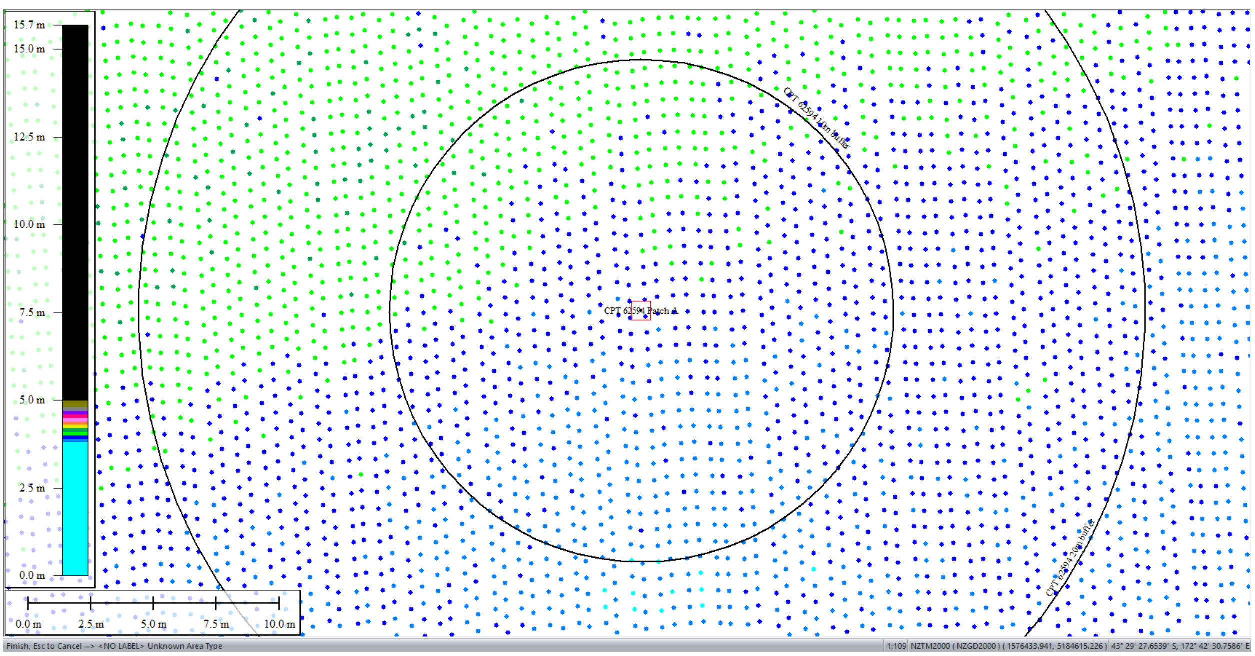

Figure 54: Ground surface elevation averaged over 10-m buffer for Patch A for Feb 2012 LiDAR survey (el. 3.953m).

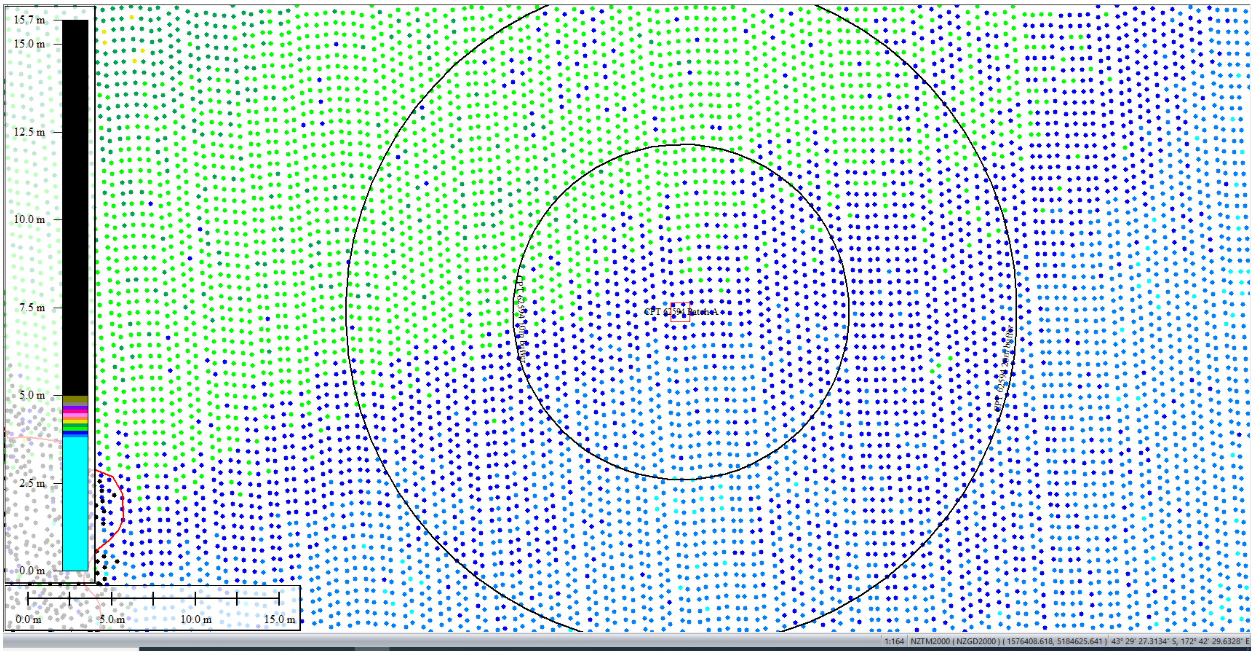

Figure 55: Ground surface elevation averaged over 20-m buffer for Patch A for Feb 2012 LiDAR survey (el. 3.968m).

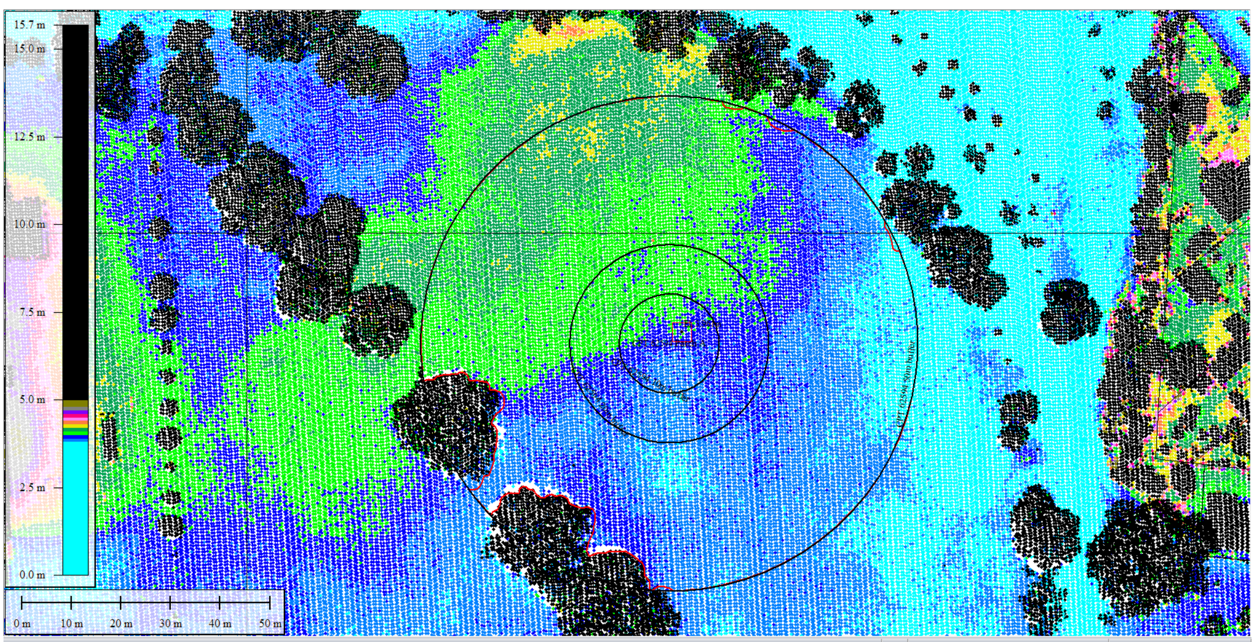

Figure 56: Ground surface elevation averaged over 50-m buffer for Patch A for Feb 2012 LiDAR survey.

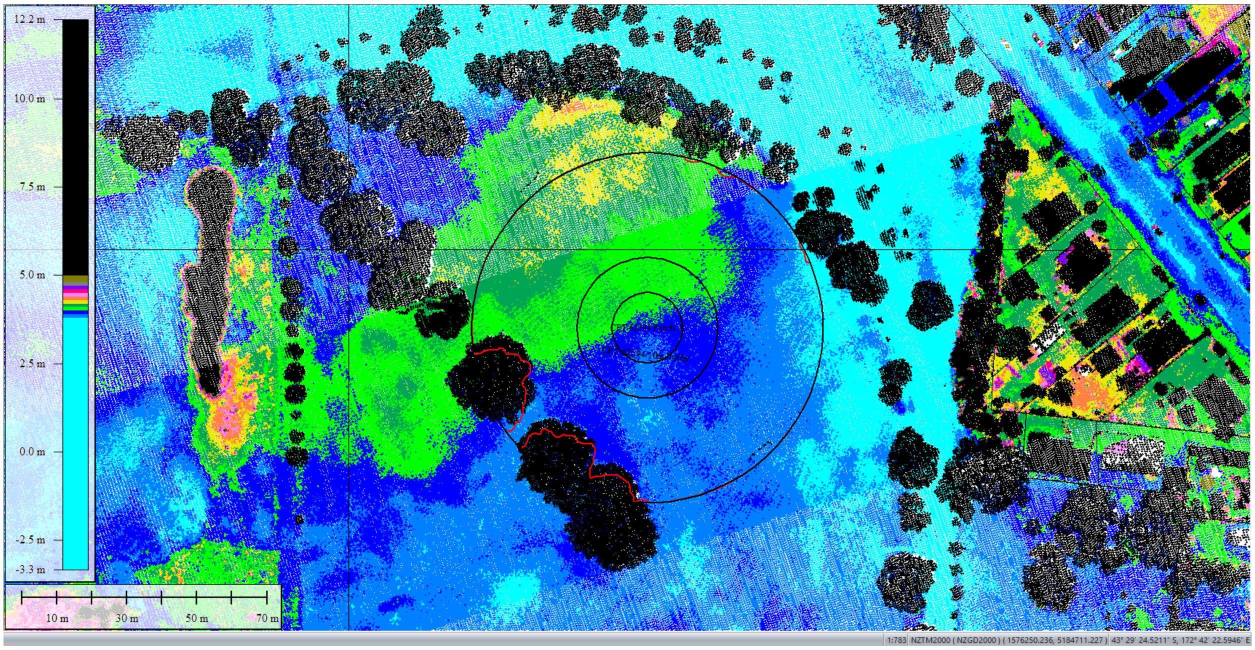

Figure 57: Oct 2015 LiDAR survey.

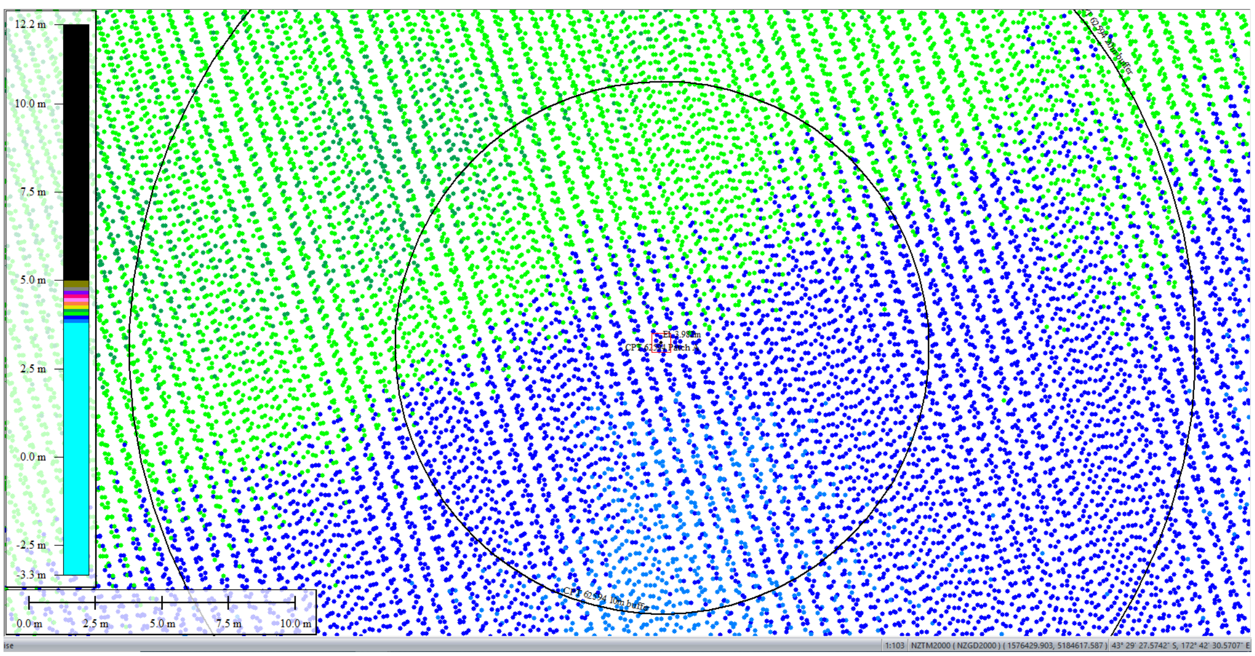

Figure 58: Ground surface elevation averaged over 10-m buffer for Patch A for Oct 2015 LiDAR survey.

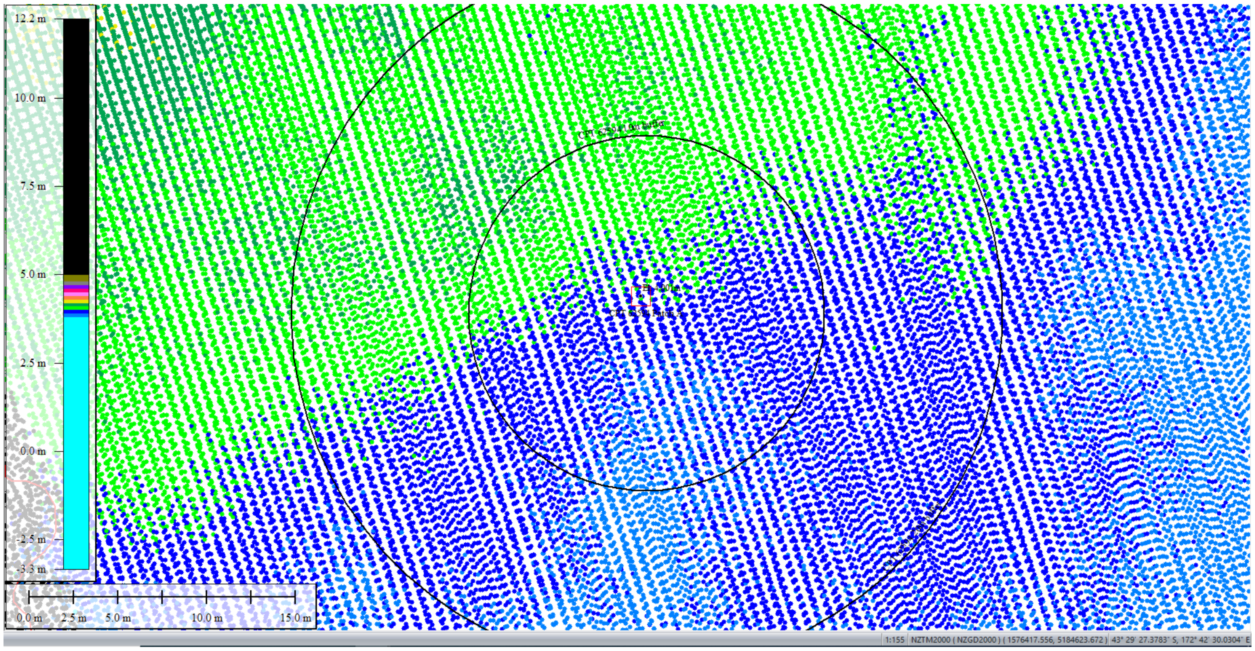

Figure 59: Ground surface elevation averaged over 20-m buffer for Patch A for Oct 2015 LiDAR survey.

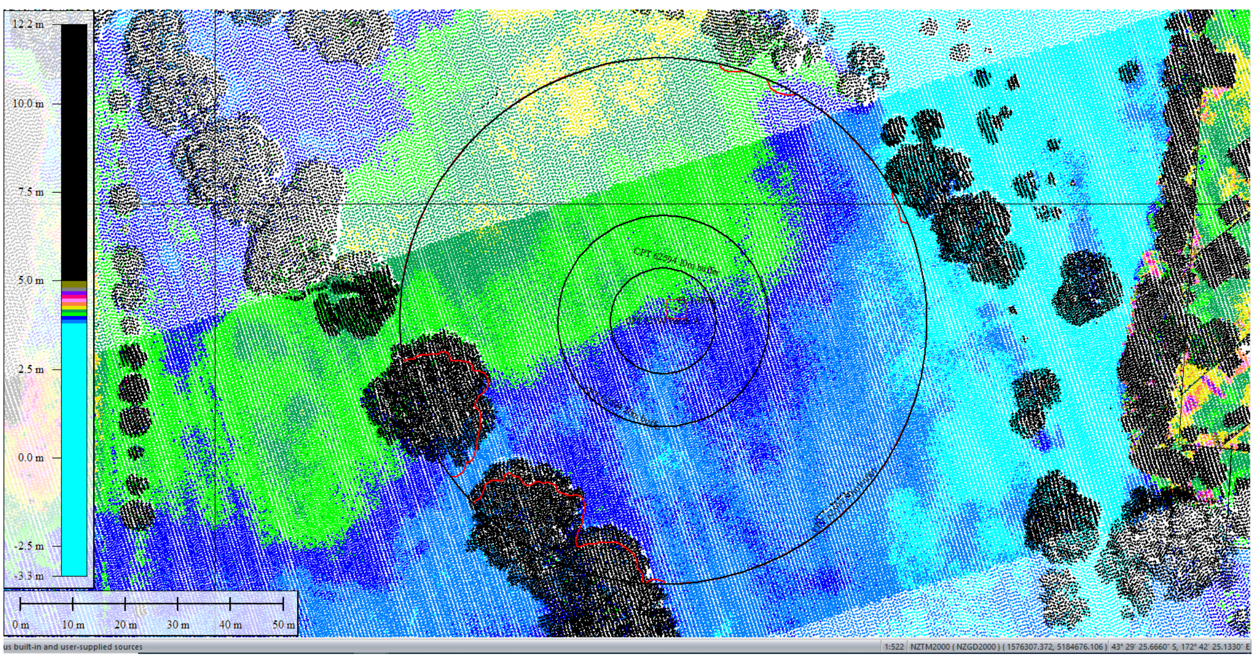

Figure 60: Ground surface elevation averaged over 50-m buffer for Patch A for Oct 2015 LiDAR survey.

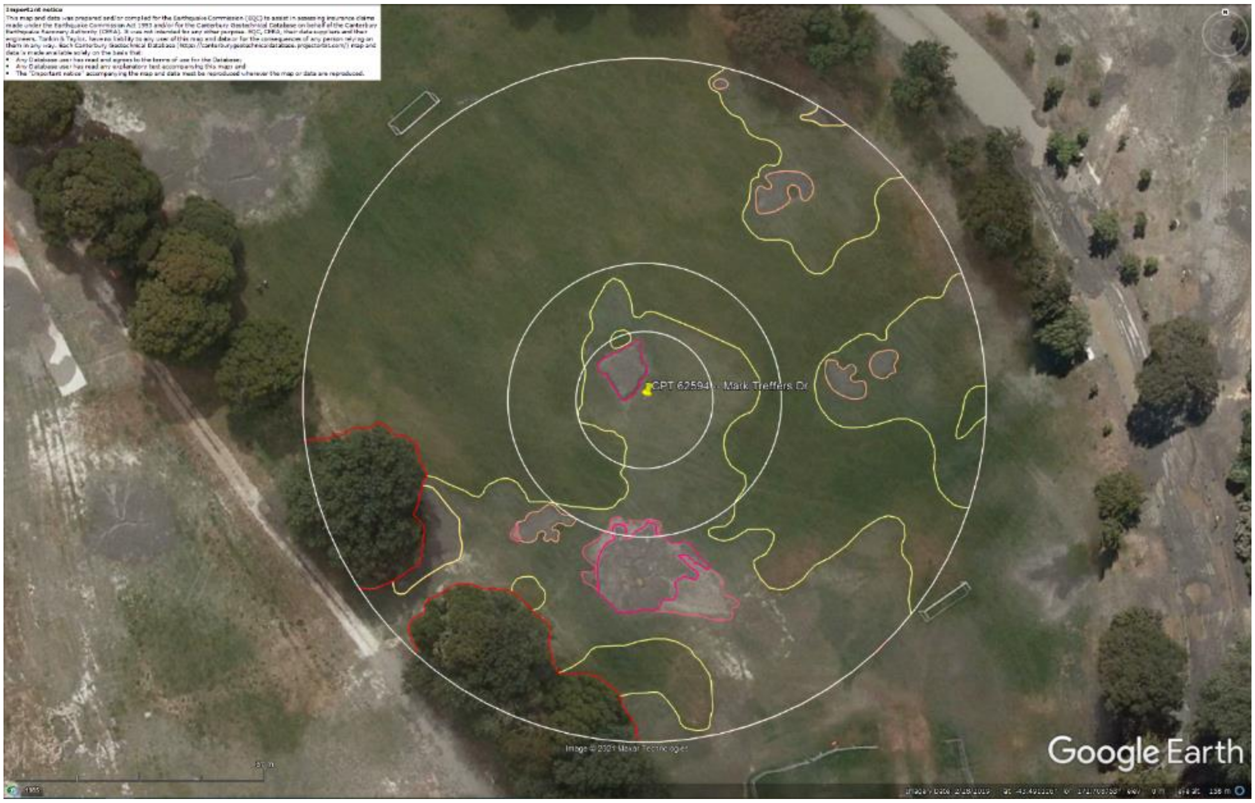

Figure 61: Aerial photograph showing the ejecta outline at the site for Feb-11 EQ.

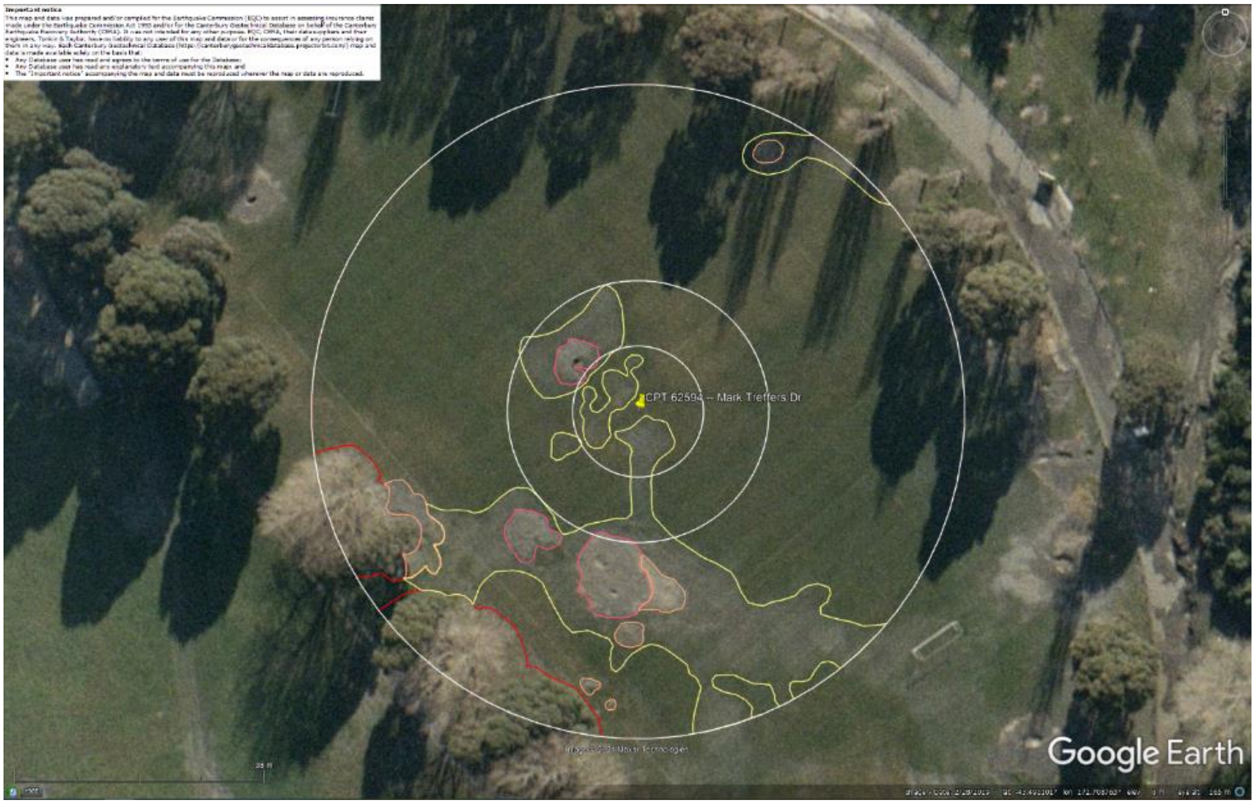

Figure 62: Aerial photograph acquired on 16 Jun 2011 showing the ejecta outline at the site for Jun-11 EQ.

Figure 63: Aerial photograph acquired on 14-15 Jun 2011 showing ejecta at the site for Jun-11 EQ.

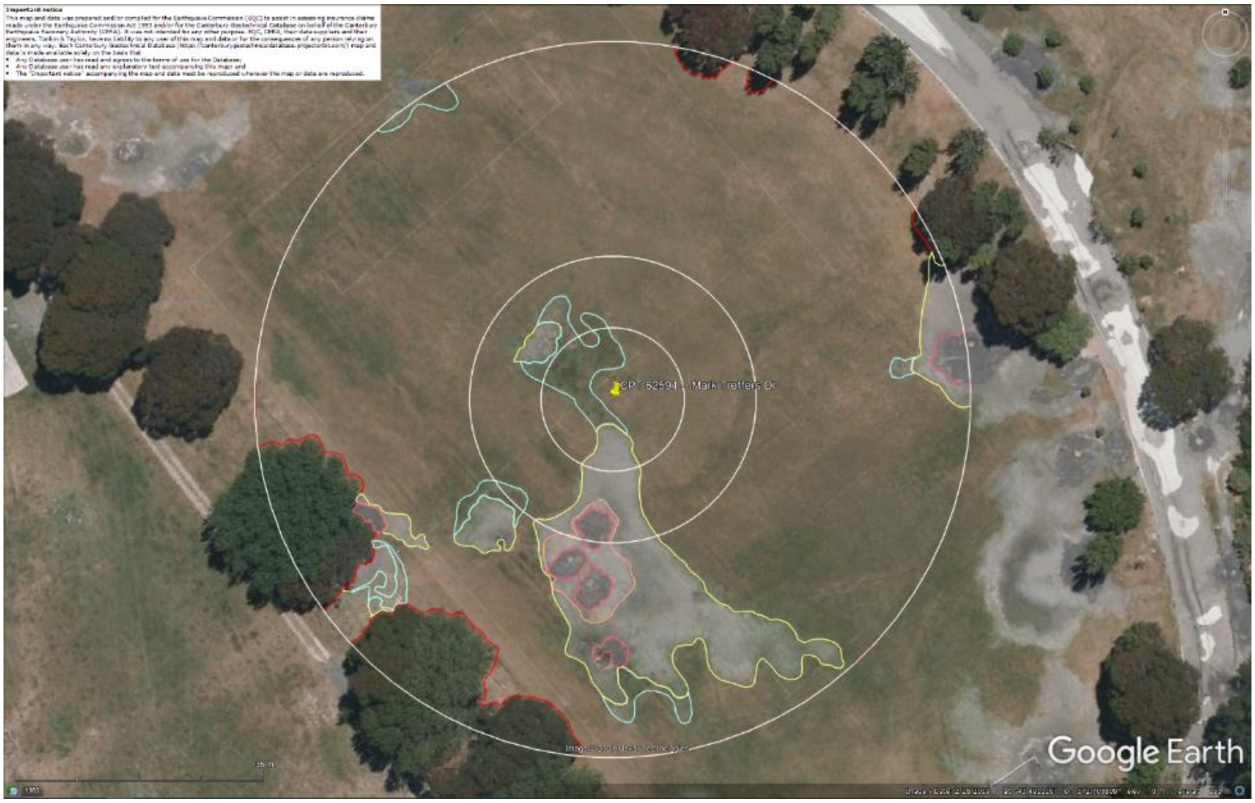

Figure 64: Aerial photograph showing the ejecta outline at the site for Dec-11 EQ.

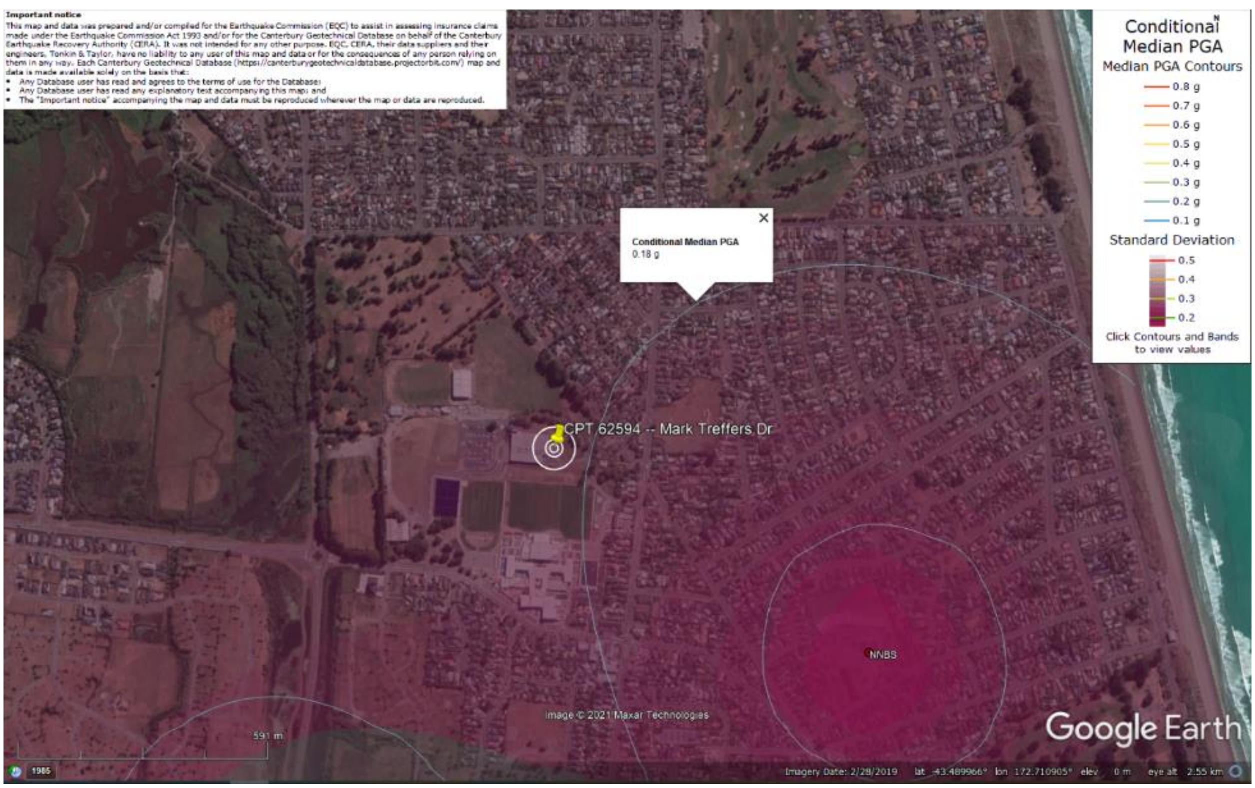

Figure 65: PGA for Sep-10 EQ (st. dev. = 0.275-0.300 ln units).

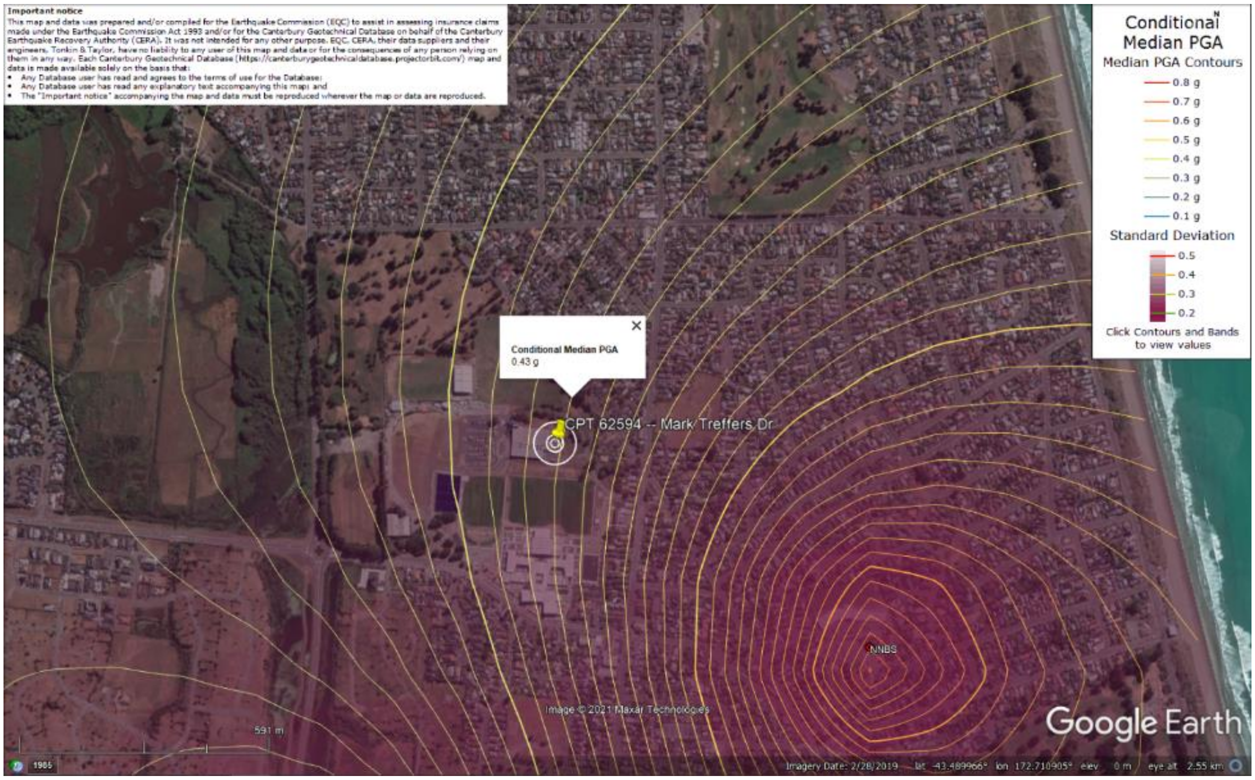

Figure 66: PGA for Feb-11 EQ (st. dev. = 0.300-0.325 ln units).

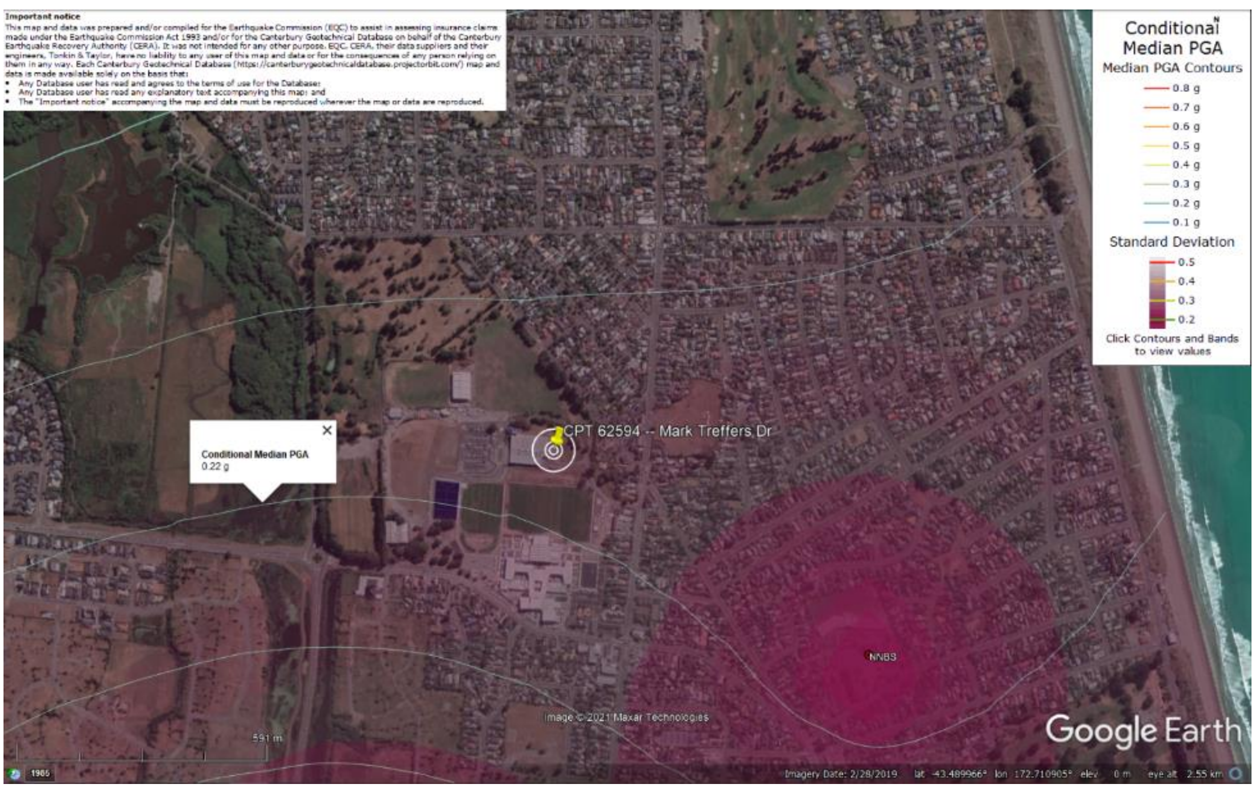

Figure 67: PGA for Jun-11 EQ (st. dev. = 0.300-0.350 ln units).

Figure 68: PGA for Dec-11 EQ (st. dev. = 0.375-0.400 ln units).

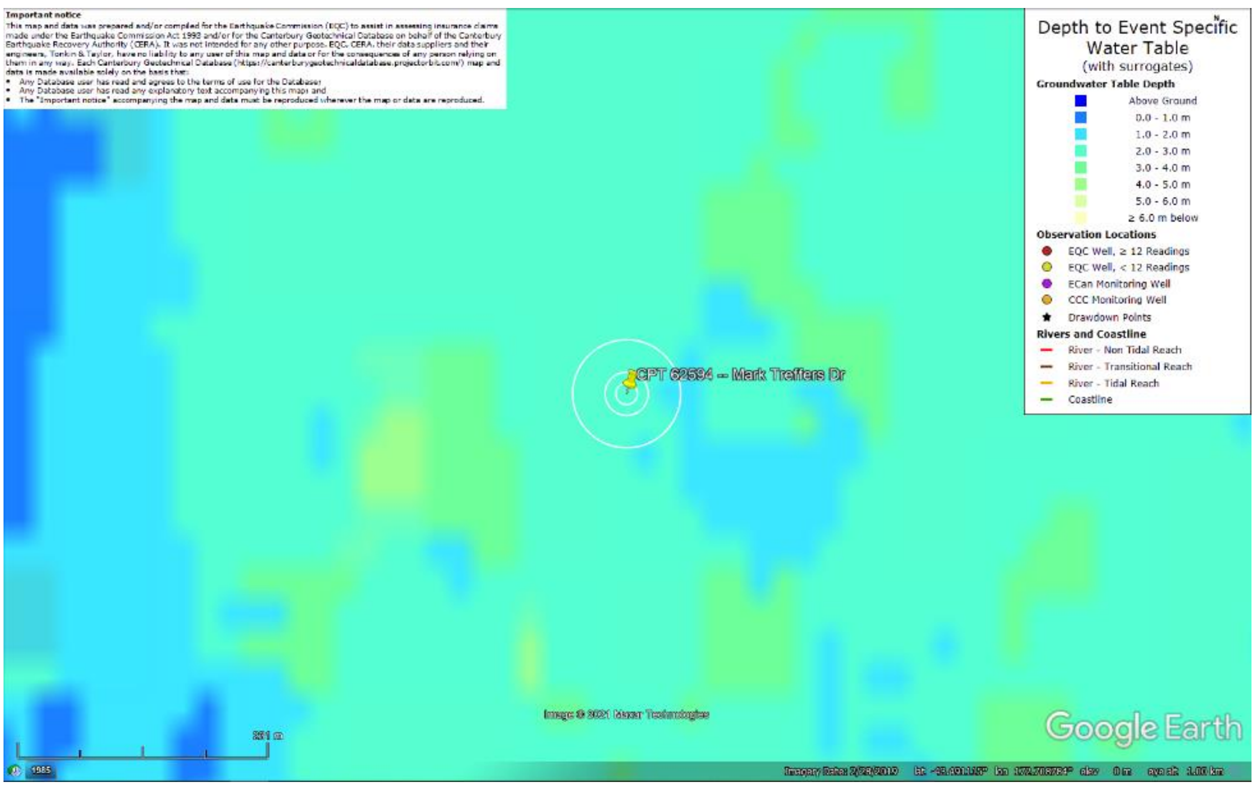

Figure 69: Depth to groundwater table for Sep-10 EQ.

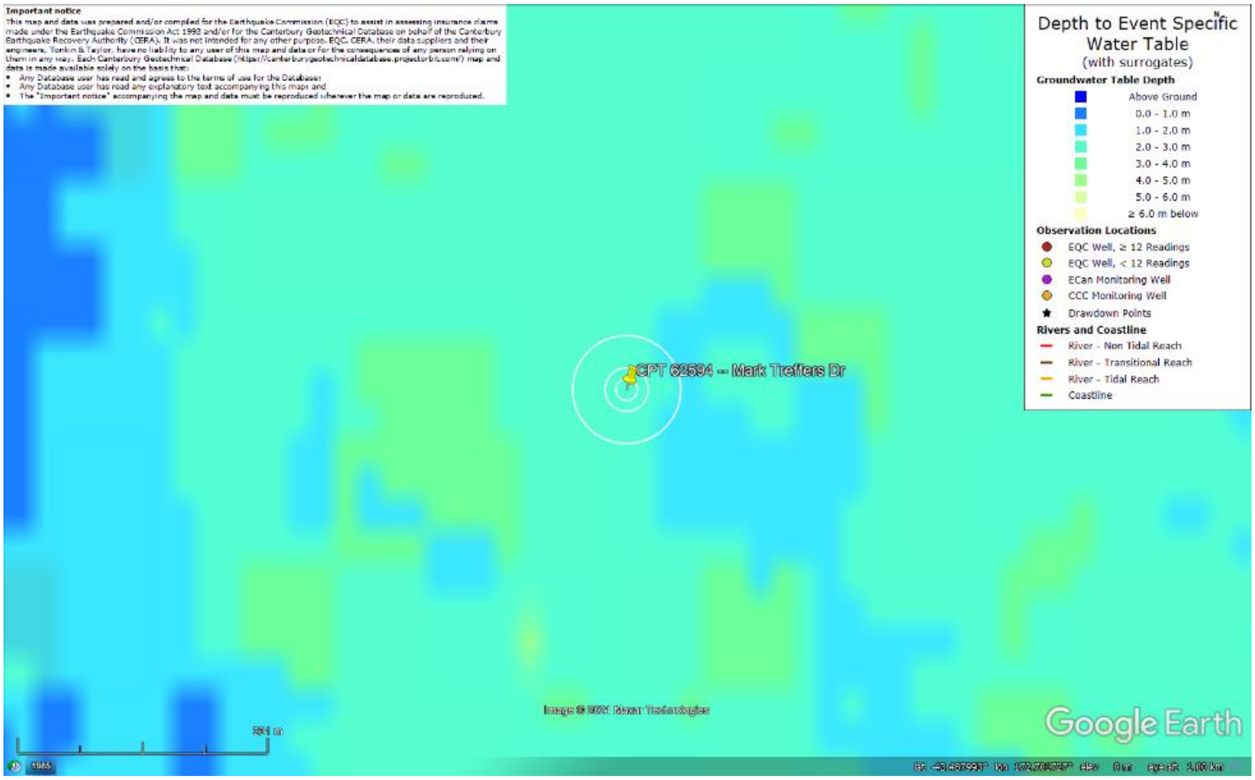

Figure 70: Depth to groundwater table for Feb-11 EQ.

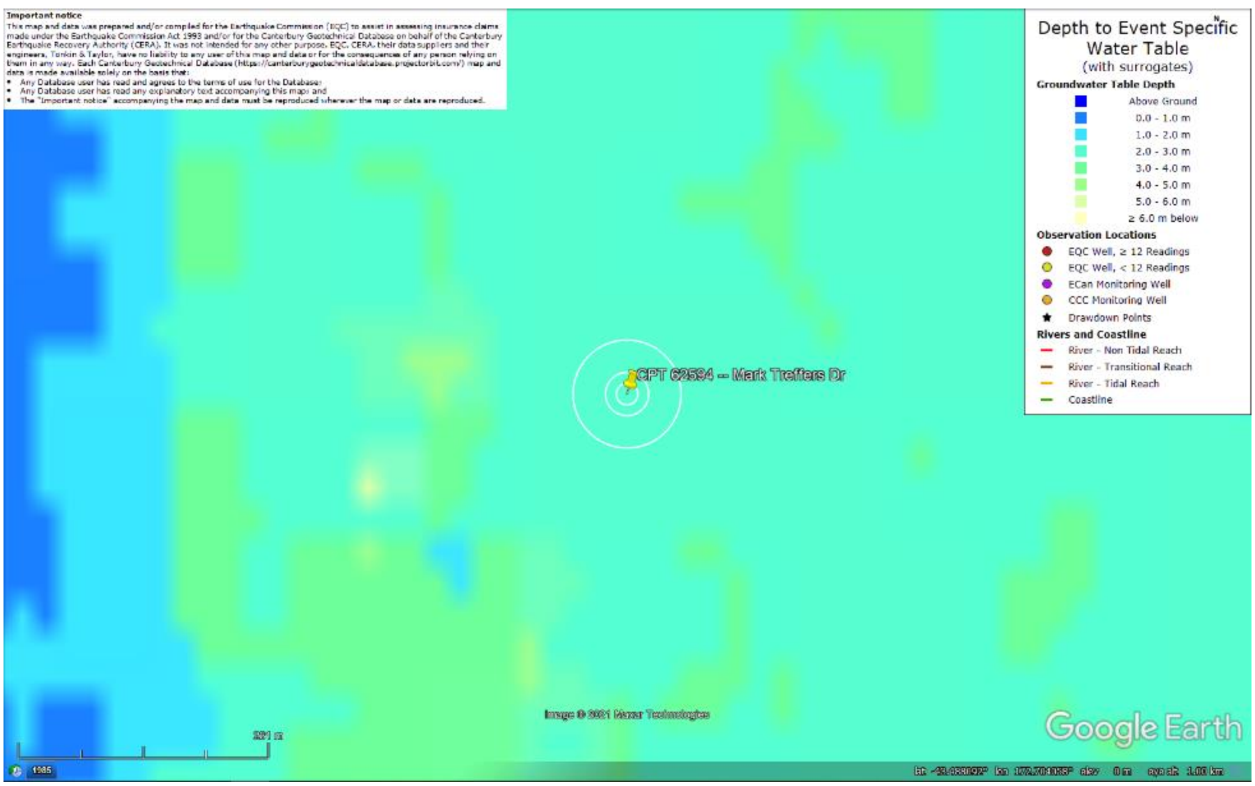

Figure 71: Depth to groundwater table for Jun-11 EQ.

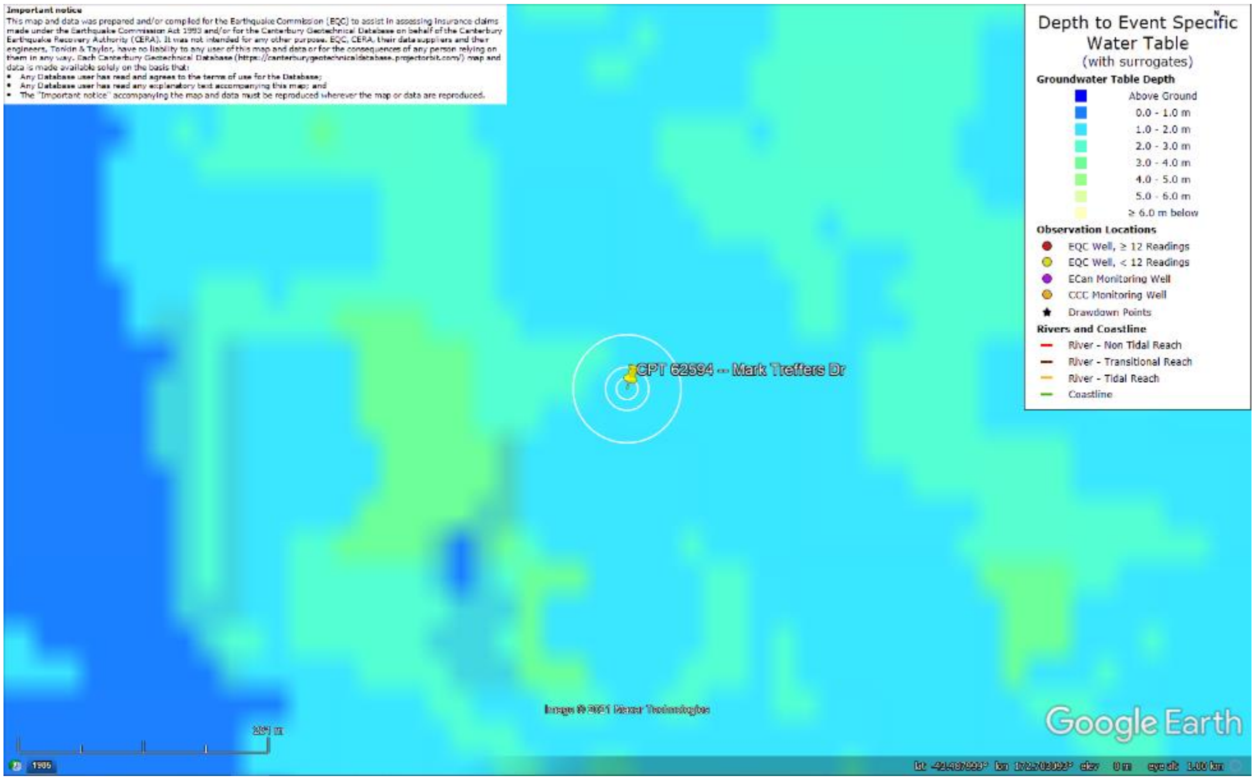

Figure 72: Depth to groundwater table for Dec-11 EQ.

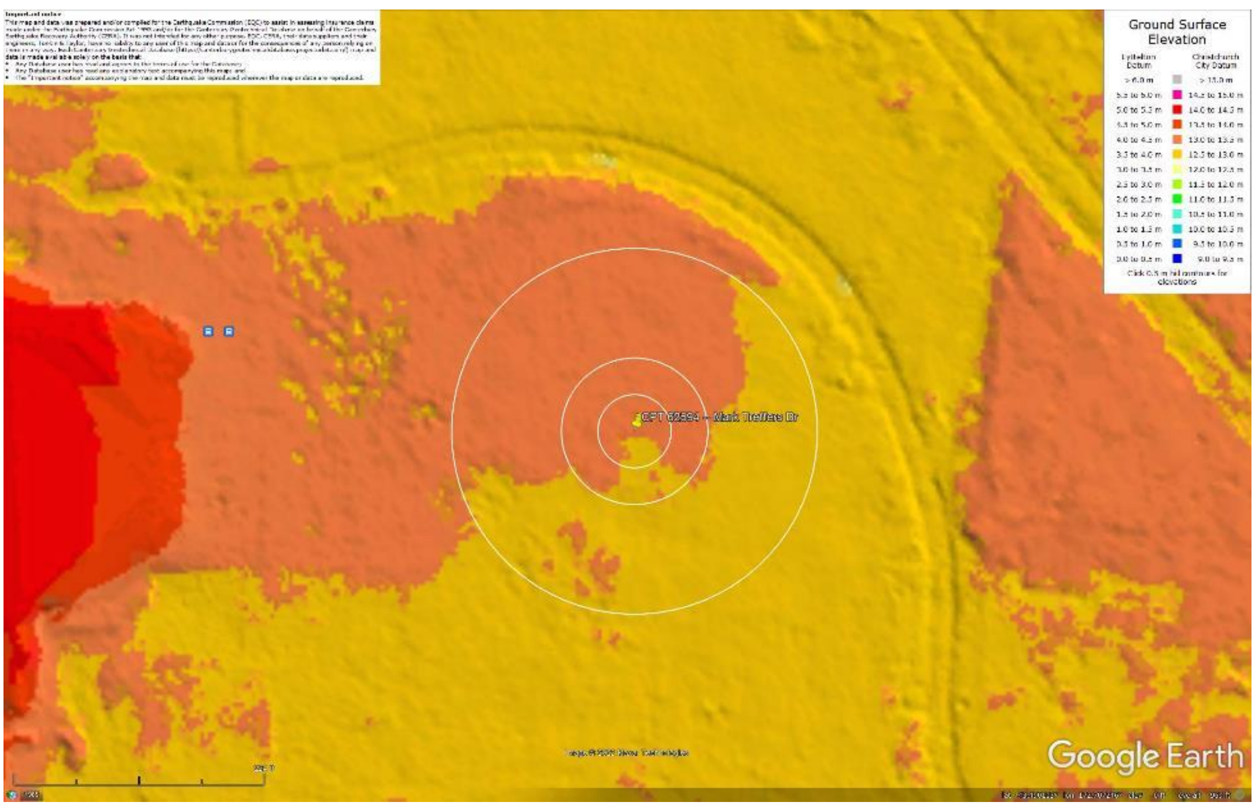

Figure 73: Ground surface elevation (Sep-11 LiDAR survey).

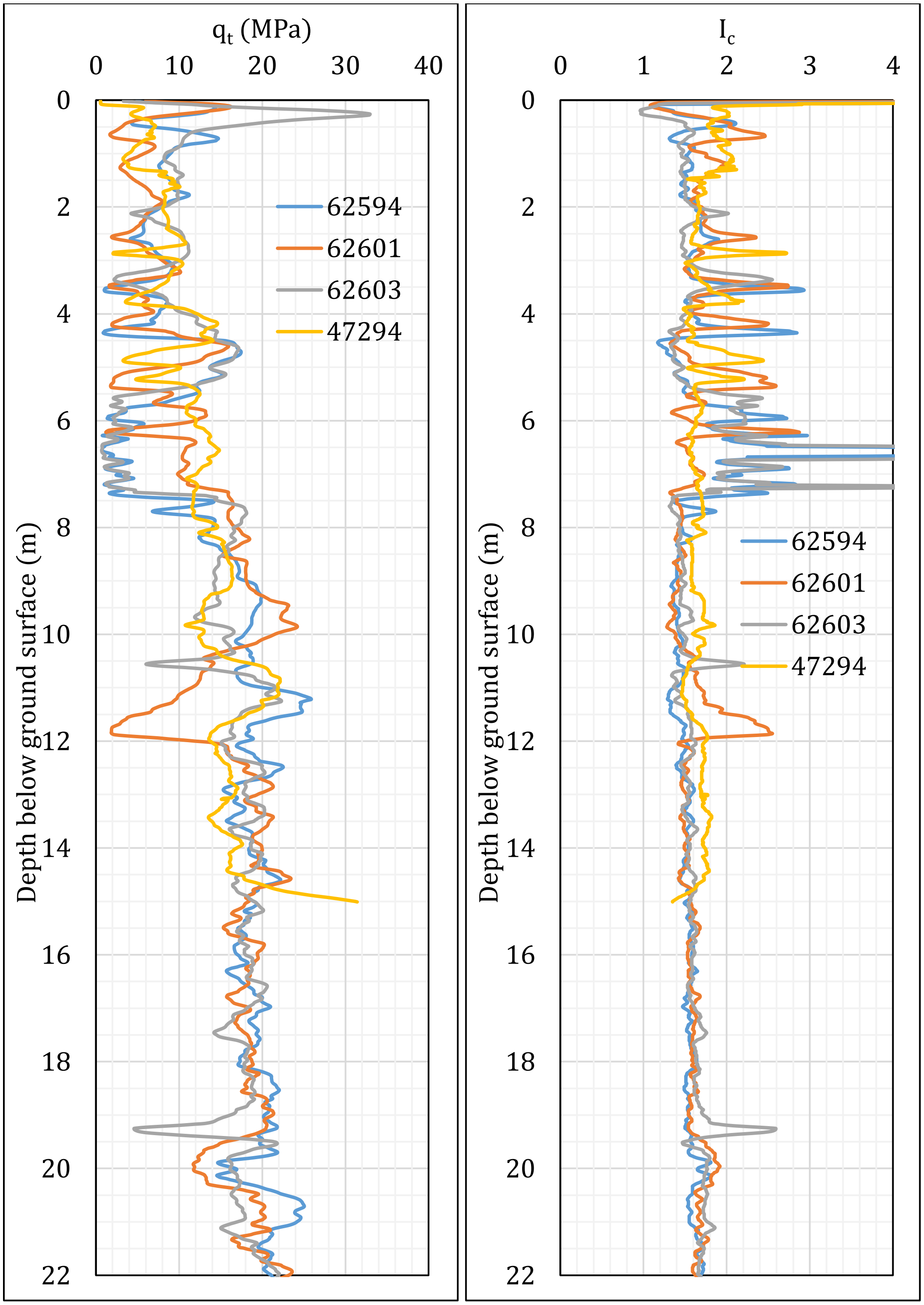

Figure 74: q_t and I_c profiles.

Note 6: The selection of CPTs for the area considered for settlement assessment (Figure 1) is based on the proximity of the CPTs to the considered areas. In accordance with that, the following table shows CPTs that were used for the volumetric settlement analysis in *Cliq v.3.0.3.2*, a CPT soil liquefaction software developed by GeoLogismiki. (The average volumetric settlements were reported in Table 8.)

Table 12: CPT profiles used in volumetric settlement analysis for areas selected for settlement assessment.

CPT ID No.	Patch A (10-m buffer)	Patch (20-m buffer)	Patch A (50-m buffer)
62594 (59240)	✓	✓	✓
62601 (59247)			✓
62603 (59249)			✓
47294			✓

Note: CPT 62594 was used to calculate the volumetric settlement for CPT 47294 for a depth range from 15 m to 20 m.

Table 13: CPT-based results.

		CPT ID				
EQ Event	Parameter	62594	62601	62603	47294	$\Delta_{15m\text{-}20m}$
Sep-10	S_{V1D} (mm)	29	23	26	1	0
	LSN	5	3	4	0	0
	LPI	1	0	1	0	0
	LPI_{ish}	0	0	0	0	--
	$D_{FS<1}$ (m)	7.22	11.5	6.14	undet.	--
Feb-11	S_{V1D} (mm)	95	127	85	57	11
	LSN	18	20	13	9	1
	LPI	10	11	8	4	0
	LPI_{ish}	7	0	5	0	--
	$D_{FS<1}$ (m)	2.68	2.52	3.14	3.50	--
Jun-11	S_{V1D} (mm)	36	30	35	1	0
	LSN	6	4	5	0	0
	LPI	1	1	1	0	0
	LPI_{ish}	0	0	0	0	--
	$D_{FS<1}$ (m)	6.06	5.18	5.82	undet.	--
Dec-11	S_{V1D} (mm)	94	119	70	41	4
	LSN	21	24	12	8	0
	LPI	10	10	7	2	0
	LPI_{ish}	7	0	2	1	--
	$D_{FS<1}$ (m)	2.06	2.1	3.14	3.54	--

Notes: $D_{FS<1}$ = Depth to the first liquefiable layer (FS_L<1) that is at least 200-mm thick, as determined by the Boulanger and Idriss (2016) liquefaction-triggering procedure (P_L=50%, C_{FC}=0.13, and $I_{c,cutoff}$ =2.6), and exported from *Cliq v.3.0.3.2*; undet. = the specified soil layer was not detected; $\Delta_{15m\text{-}20m}$ indicates the amount of S_{V1D}, LSN, and LPI to be added to CPT 47294 due to its penetration depth being shallower than 20 m.

Note 7: Based on the nearest borehole log (BH 3642, ~140 m to the E from the center of the site), the groundwater table is at a depth of 1. 5 m below the ground surface. At that location, the soil profile consists of (1) fine to medium sand, SP, to a depth of 4.3 m, (2) silty sand, SM, to a depth of 4.6 m, and (3) fine to medium sand, SP, to a depth of 20 m. All soil layers are of the Christchurch formation. The borehole log BH 3642 (~140 m to the NE from the center of the site) indicates that the groundwater table is at a depth of 2.5 m below the ground surface and that the soil deposit is comprised predominantly of thick, clean sand, SP, with a silty fine to medium sand, SM, layer at a depth range from 3.7 m to 5.8 m. According to CPTs 62594 and 62603, there is a silt layer from a 5.7-m depth to a 7.5-m depth.

Note 8: The ejecta-induced free-field settlement provided in Table 11 is an areal average settlement due to ejecta, which is based on the total settlement assessment area, A_T (provided in Table 9 and repeated in Table 14). However, the considered area was not always covered completely with ejecta; thus, it is important to provide the localized ejecta-induced settlement, too. The localized settlement due to ejecta is estimated using photographic evidence only as

$$S_{E,P\_localized} = \frac{V_E}{A_E}$$

where V_E is the total volume of ejecta within A_T and A_E is the total coverage area of ejecta within A_T. Please note that the areal ejecta-induced settlement provided in Table 14 as S_{E,P_areal} is the same as $S_{E,P}$ in Table 11, which was estimated as

$$S_{E,P\_areal} = S_{E,P} = \frac{V_E}{A_T}$$

where V_E is the total volume of ejecta within A_T and A_T is the total settlement assessment area.

Table 14a: Areal and localized ejecta-induced settlement estimates for Patch A (10-m buffer) based on photographic evidence.

Earthquake Event	A_T (m^2)	A_E (m^2)	V_E (m^3)	S_{E,P_areal} (mm)	$S_{E,P\_localized}$ (mm)
Sep-10	314	0	0	0	0
Feb-11	314	283	5.9-10.4	25±5	30±10
Jun-11	314	112	1.2-2.3	5±5	15±5
Dec-11	314	109	0.6-1.5	5±5	10±5

Notes: S_{E,P_areal} = $S_{E,P}$ reported in Table 11 = areal ejecta-induced settlement; $S_{E,P\_localized}$ = localized ejecta-induced settlement; A_T = total settlement assessment area; V_E = total volume of ejecta within A_T; A_E = total area of ejecta within A_T; The estimates of both areal and localized ejecta-induced settlement are rounded to the nearest 5; Final plus/minus values are also rounded to the nearest 5.

Table 14b: Areal and localized ejecta-induced settlement estimates for Patch A (20-m buffer) based on photographic evidence.

Earthquake Event	A_T (m^2)	A_E (m^2)	V_E (m^3)	S_{E,P_areal} (mm)	$S_{E,P\_localized}$ (mm)
Sep-10	1257	0	0	0	0
Feb-11	1257	640	10.4-19.0	10±5	25±5
Jun-11	1257	328	5.1-9.5	5±5	25±5
Dec-11	1257	277	3.3-7.8	5±5	20±10

Notes: S_{E,P_areal} = $S_{E,P}$ reported in Table 11 = areal ejecta-induced settlement; $S_{E,P\_localized}$ = localized ejecta-induced settlement; A_T = total settlement assessment area; V_E = total volume of ejecta within A_T; A_E = total area of ejecta within A_T; The estimates of both areal and localized ejecta-induced settlement are rounded to the nearest 5; Final plus/minus values are also rounded to the nearest 5.

Table 14c: Areal and localized ejecta-induced settlement estimates for Patch A (50-m buffer) based on photographic evidence.

Earthquake Event	A_T (m^2)	A_E (m^2)	V_E (m^3)	S_{E,P_areal} (mm)	$S_{E,P\_localized}$ (mm)
Sep-10	7107	0	0	0	0
Feb-11	7107	2885	54.5-97.5	10±5	25±5
Jun-11	7283	1437	26.2-48.6	5±5	25±10
Dec-11	7107	1085	17.8-41.8	5±5	30±10

Notes: S_{E,P_areal} = $S_{E,P}$ reported in Table 11 = areal ejecta-induced settlement; $S_{E,P\_localized}$ = localized ejecta-induced settlement; A_T = total settlement assessment area; V_E = total volume of ejecta within A_T; A_E = total area of ejecta within A_T; The estimates of both areal and localized ejecta-induced settlement are rounded to the nearest 5; Final plus/minus values are also rounded to the nearest 5.

<u>Summary 2:</u>

The best estimate of the <u>localized</u> ejecta-induced free-field ground settlement at the Mark Treffers Dr site for the SEP 2010, FEB 2011, JUN 2011, and DEC 2011 earthquake is 0 mm, 30±10 mm, 15±5 mm, and 10±5 mm, respectively.